HEPATOLOGY

Massive rearrangements of cellular miRNA signatures are key drivers of hepatocyte dedifferentiation

Journal:	*Hepatology*
Manuscript ID	HEP-16-0352.R2
Wiley - Manuscript type:	Original
Date Submitted by the Author:	n/a
Complete List of Authors:	Lauschke, Volker; Karolinska Institutet Department of Physiology and Pharmacology, Vorrink, Sabine; Karolinska Institutet Department of Physiology and Pharmacology Moro, Sabrina; Karolinska Institutet, Physiology and Pharmacology Rezayee, Fatemah; Karolinska Institutet Department of Physiology and Pharmacology Nordling, Åsa; Karolinska Institutet Department of Physiology and Pharmacology Hendriks, Delilah; Karolinska Institutet, Physiology and Pharmacology Bell, Catherine; Karolinska Institutet, Physiology and Pharmacology Sison-Young, Rowena; MRC Centre for Drug Safety Science, Department of Molecular and Clinical Pharmacology Park, B.Kevin; MRC Centre for Drug Safety Science, Department of Molecular and Clinical Pharmacology Goldring, Chris; University of Liverpool, Pharmacology and Therapeutics Ellis, Ewa; Karolinska Institute, Clinical sciences, Intervention and Technology Johansson, Inger; Karolinska Institutet Department of Physiology and Pharmacology Mkrtchian, Souren; Karolinska Institutet Department of Physiology and Pharmacology Andersson, Tommy; Karolinska Institutet Department of Physiology and Pharmacology; AstraZeneca, Innovative Medicines Ingelman-Sundberg, Magnus; Karolinska Institutet, Physiology and Pharmacology
Keywords:	miRNA, primary human hepatocytes, transcriptomics, cytochrome P450, drug metabolism

Title: Massive rearrangements of cellular miRNA signatures are key drivers of hepatocyte dedifferentiation

Volker M. Lauschke[1]*, Sabine U. Vorrink[1], Sabrina M. Moro[1], Fatemah Reyazee[1], Åsa Nordling[1], Delilah F. Hendriks[1], Catherine C. Bell[1], Rowena Sison-Young[2], B. Kevin Park[2], Christopher E. Goldring[2], Ewa Ellis[3], Inger Johansson[1], Souren Mkrtchian[1], Tommy B. Andersson[1,4] and Magnus Ingelman-Sundberg[1]

[1] Section of Pharmacogenetics, Department of Physiology and Pharmacology, Karolinska Institutet, SE-17177 Stockholm, Sweden.

[2] MRC Centre for Drug Safety Science, Department of Molecular and Clinical Pharmacology, Sherrington Buildings, Ashton Street, University of Liverpool, UK.

[3] Department of Clinical Science, Intervention and Technology, Karolinska University Hospital Huddinge, Karolinska Institutet, Stockholm, Sweden

[4] Cardiovascular and Metabolic Diseases Innovative Medicines, DMPK, AstraZeneca R&D, SE-431 83, Mölndal, Sweden

* To whom correspondence should be addressed

Volker M. Lauschke, Karolinska Institutet, Department of Physiology and Pharmacology, Section of Pharmacogenetics, Nanna Svartz Väg 2, 17177 Stockholm, Sweden, Phone: +46 8524 87711, Fax: +46 8337 327, E-mail: volker.lauschke@ki.se

Sabine U. Vorrink, Karolinska Institutet, Department of Physiology and Pharmacology, Section of Pharmacogenetics, Nanna Svartz Väg 2, 17177 Stockholm, Sweden, Phone: +46 8524 87762, Fax: +46 8337 327, E-mail: sabine.vorrink@ki.se

Sabrina M. L. Moro, Karolinska Institutet, Department of Physiology and Pharmacology, Section of Pharmacogenetics, Nanna Svartz Väg 2, 17177 Stockholm, Sweden, Phone: +46 8524 87762, Fax: +46 8337 327, E-mail: sabrina.ml.moro@gmail.com

Fatemah Reyazee, Karolinska Institutet, Department of Physiology and Pharmacology, Section of Pharmacogenetics, Nanna Svartz Väg 2, 17177 Stockholm, Sweden, Phone: +46 8524 87711, Fax: +46 8337 327, E-mail: fatemah.rezayee@hotmail.se

Åsa Nordling, Karolinska Institutet, Department of Physiology and Pharmacology, Section of Pharmacogenetics, Nanna Svartz Väg 2, 17177 Stockholm, Sweden, Phone: +46 8524 87762, Fax: +46 8337 327, E-mail: asa.nordling@ki.se

Delilah F. G. Hendriks, Karolinska Institutet, Department of Physiology and Pharmacology, Section of Pharmacogenetics, Nanna Svartz Väg 2, 17177 Stockholm, Sweden, Phone: +46 8524 87711, Fax: +46 8337 327, E-mail: delilah.hendriks@ki.se

Catherine Bell, Karolinska Institutet, Department of Physiology and Pharmacology, Section of Pharmacogenetics, Nanna Svartz Väg 2, 17177 Stockholm, Sweden, Phone: +46 8524 87711, Fax: +46 8337 327, E-mail: catherine.bell@ki.se

Rowena Sison-Young, MRC Centre for Drug Safety Science, Department of Molecular and Clinical Pharmacology, Sherrington Buildings, Ashton Street, University of Liverpool, Liverpool, L69 3GE, UK. Email: rowena.sison-young@liverpool.ac.uk

B. Kevin Park, MRC Centre for Drug Safety Science, Department of Molecular and Clinical Pharmacology, Sherrington Buildings, Ashton Street, University of Liverpool, Liverpool, L69 3GE, UK. Email: B.K.Park@liverpool.ac.uk

Christopher E.P. Goldring, MRC Centre for Drug Safety Science, Department of Molecular and Clinical Pharmacology, Sherrington Buildings, Ashton Street, University of Liverpool, Liverpool, L69 3GE, UK. Email: chrissy@liv.ac.uk

Ewa Ellis, Department of Clinical Science, Intervention and Technology, Karolinska University Hospital Huddinge, Karolinska Institutet, Stockholm, Sweden E mail: ewa.ellis@ki.se

Inger Johansson, Karolinska Institutet, Department of Physiology and Pharmacology, Section of Pharmacogenetics, Nanna Svartz Väg 2, 17177 Stockholm, Sweden, Phone: +46 8524 87762, Fax: +46 8337 327, E-mail: inger.johansson@ki.se

Souren Mkrtchian, Karolinska Institutet, Department of Physiology and Pharmacology, Section of Pharmacogenetics, Nanna Svartz Väg 2, 17177 Stockholm, Sweden, Phone: +46 8524 87762, Fax: +46 8337 327, E-mail: souren.mkrtchian@ki.se

Tommy B. Andersson, AstraZeneca, R&D, Cardiovascular and Metabolic Diseases, Innovative Medicines and Early Development Biotech Unit, Pepparedsleden 1, 43183 Mölndal, Sweden, Phone: +46 317761534, Fax: +46 317763786, Email: tommy.b.andersson@astrazeneca.com

Magnus Ingelman-Sundberg, Karolinska Institutet, Department of Physiology and Pharmacology, Section of Pharmacogenetics, Nanna Svartz Väg 2, 17177 Stockholm, Sweden, Phone: +46 8524 877 35, Fax: +46 8337 327, E-mail: magnus.ingelman-sundberg@ki.se

Corresponding author: Volker M. Lauschke, Karolinska Institutet, Department of Physiology and Pharmacology, Section of Pharmacogenetics, Nanna Svartz Väg 2, 17177 Stockholm, Sweden, Phone: +46 8524 87711, Fax: +46 8337 327, E-mail: volker.lauschke@ki.se

List of Abbreviations: PHH: primary human hepatocytes; CYP: cytochrome P450; ncRNA: non-coding RNA; miRNA: micro RNA; snoRNA: small nucleolar RNA; lncRNA: long non-coding RNA; RISC: RNA-induced silencing complex; ADME: absorption, distribution, metabolism and excretion; AF: acriflavine; PLL: poly-L-lysine.

Keywords: miRNA, transcriptomics, primary human hepatocytes, cytochrome P450, drug metabolism

Conflict of interest: V.M.L. and M.I.-S. are founders and owners of HepaPredict AB.

Financial support: This work was supported by grants from AstraZeneca, The Swedish Research Council and by the European Community under the Innovative

Medicine Initiative project MIP-DILI [grant agreement number 115336]. V.M.L. was supported by a MarieCurie IEF fellowship for career development in the context of the European FP7 framework program and by a grant from the Eva och Oscar Ahrèns Stiftelse.

Electronic Word Count: 5994 words

Abstract

Hepatocytes are dynamic cells that upon injury can alternate between non-dividing differentiated and dedifferentiated proliferating states *in vivo*. However, in 2D cultures primary human hepatocytes rapidly dedifferentiate resulting in the loss of hepatic functions which significantly limits their usefulness as *in vitro* model of liver biology, liver diseases as well as drug metabolism and toxicity. Thus, understanding the underlying mechanisms and stalling of the dedifferentiation process would be highly beneficial to establish more accurate and relevant long-term *in vitro* hepatocyte models. Here, we present comprehensive analyses of whole proteome and transcriptome dynamics during the initiation of dedifferentiation during the first 24 hours of culture. We report that early major rearrangements of the non-coding transcriptome, hallmarked by increased expression of snoRNAs, lncRNAs, miRNAs, and ribosomal genes, precede most changes in coding genes during dedifferentiation of primary human hepatocytes and we speculated that these modulations could drive the hepatic dedifferentiation process. To functionally test this hypothesis, we globally inhibited the miRNA machinery using two established chemically-distinct compounds, acriflavine and poly-L-lysine. These inhibition experiments resulted in a significantly impaired miRNA response and, most importantly, in a pronounced reduction in the downregulation of hepatic genes with importance for liver function. Thus, we provide strong evidence for the importance of ncRNAs, in particular miRNAs, in hepatic dedifferentiation, which can aid the development of more efficient differentiation protocols for stem cell-derived hepatocytes and broaden our understanding of the dynamic properties of hepatocytes with respect to liver regeneration.

Conclusion: miRNAs are important drivers of hepatic dedifferentiation and our results provide valuable information regarding the mechanisms behind liver regeneration and possibilities to inhibit dedifferentiation *in vitro*.

Introduction

Upon liver injury, hepatic cells proliferate and rapidly regenerate large parts of the damaged organ *in vivo*[1]. Different mechanisms of liver regeneration have been described in different injury models. Under most injuries, such as partial hepatectomy, the liver regenerates by self-duplication of hepatocytes[2]. Yet, when hepatocyte proliferation is compromised, the formation of duct-like "oval cells" with a mixed mesenchymal and epithelial expression signature has been observed[3]. These progenitor cells are assumed to originate from the terminal branches of the intrahepatic biliary system[4] and seminal work demonstrated that these cells can give rise to hepatocytes[5]. Yet, recent studies in mouse models of chronic liver insults indicated that new hepatocytes originated from pre-existing hepatocytes rather than from distinguished non-parenchymal stem-cell populations[6,7]. One explanation for this ostensible discrepancy might be the capacity of hepatocytes to undergo reversible ductal metaplasia, which opens the possibility that hepatocyte-derived progenitor cells expressing biliary markers are mistaken for progenitor cells of biliary origin[8,9].

In vitro in 2D monolayer cultures, primary human hepatocytes (PHH) rapidly lose their phenotype and dedifferentiate into fetal-like progenitor states with drastically reduced liver-specific functionality, which hampers their usefulness for studies of liver biology, liver disease, drug metabolism and toxicity[10,11]. Most importantly, PHH rapidly lose expression of important liver-specific genes, such as cytochrome P450 (CYP) enzymes, phase 2 enzymes and transporters[12]. Therefore, decipherment and eventual inhibition of the dedifferentiation process could allow for more accurate and relevant long-term *in vitro* hepatocyte models. Furthermore, mechanistic

understanding of the dedifferentiation process can guide the development of more efficient differentiation protocols for stem cell-derived hepatocytes. Until now however, the molecular cues that initiate the dedifferentiation process and its mediators that render hepatocytes capable to respond so rapidly to a changing cellular environment have remained elusive.

Changes in transcript levels can be modulated by non-coding (nc)RNA species such as micro (mi)RNAs, small nucleolar (sno)RNAs, and long non-coding (lnc)RNAs[13]. miRNAs are short single-stranded RNAs that associate with the RNA-induced silencing complex (RISC) by binding to AGO proteins, downregulating protein output of complementary transcripts by translational inhibition or transcript degradation[14]. An *in silico* study using 79 human livers showed that levels of 275 miRNAs correlated inversely with expression patterns of their putative hepatic target genes[15]. Furthermore, analyses of miRNA expression during the differentiation of stem cells to hepatocyte-like cells implicated dozens of miRNAs in these developmental programs[16]. Yet, miRNA dynamics during hepatocyte dedifferentiation remain to be elucidated. Combined, these data suggest that miRNAs are of paramount importance for liver function and hepatic differentiation and merit detailed investigation.

snoRNAs guide modifications of other ncRNA species such as ribosomal RNAs, thereby contributing to the remodeling of the cell's translational capabilities[17,18]. Furthermore, many snoRNAs harbor sno-derived (sd)RNAs that are commonly conserved across species from vertebrates to plants[19]. Interestingly, some sdRNAs have been shown to impact alternative splicing and are implicated in disease (e.g.

SNORD115 in Prader-Willi syndrome[20]), while others control levels of target mRNAs[21,22].

lncRNAs are a rapidly growing class of ncRNAs that can influence protein output by regulating transcription of nearby or distal genes, impacting splicing, RNA stability or translation, as well as acting as miRNA decoys (see [23] and references therein). lncRNAs are difficult to study *en bloc* because (i) they cannot be predicted solely on their sequence and (ii) the functionality and molecular mode of action of most lncRNA family members remains poorly understood.

While mounting evidence indicates important roles for ncRNAs in hepatic dedifferentiation, their dynamics and functional effects have not been quantitatively assessed with high temporal resolution. Therefore, we here thoroughly characterized changes in coding and non-coding transcriptomes during dedifferentiation of PHH using unsupervised whole transcriptome analyses. We detected massive alterations of ncRNA signatures that preceded changes in coding transcripts during later stages of dedifferentiation. In order to investigate whether these ncRNA modulations could drive the dedifferentiation process, we established a miRNA inhibition assay using two chemically-distinct inhibitors that interfere with different nodes of the miRNA-processing pathway. We found that miRNA inhibition significantly reduced the early miRNA response and the loss of hepatic marker genes. Moreover, whole-transcriptome analyses revealed that gene expression changes during dedifferentiation in inhibitor-treated samples were globally reduced, thus providing strong evidence for the importance of ncRNAs, in particular miRNAs, in hepatic dedifferentiation.

Materials and Methods

Hepatocytes cultures

Fresh hepatocytes obtained from patients subject to liver resections at Huddinge University Hospital, Stockholm, Sweden were used for the dedifferentiation experiments (Table 1). The hepatocytes obtained from patient livers were isolated as previously described[24]. Use of liver specimens was approved by the Ethics Committee at Karolinska Institutet and written informed consent was obtained from all donors of liver material. Hepatocytes were seeded into plates coated with 5 µg/cm^2 Rat Tail Collagen Type I (Corning) in culture medium (Williams E medium supplemented with 2mM L-glutamine, 100 units/ml penicillin, 100 µg/ml streptomycin, 10 µg/ml insulin, 5.5 µg/ml transferrin, 6.7 ng/ml sodium selenite, 100nM dexamethasone) with 10% FBS. After two hours of attachment, the medium was replaced with serum-free culture medium. Time point 0 (t0) is defined as immediately before plating. The other time points denote time passed since plating.

miRNA inhibition experiments

Cryopreserved hepatocytes were thawed according to the supplier's protocol (BioreclamationIVT) and cultured as above. Cells were treated with 2 (low), 10 (medium) or 30 µM (high) AF or 1 (low), 5 (medium) or 15 µM (high) PLL as indicated.

Statistical analyses

Unsupervised hierarchical clustering and principal component analysis of genes was performed in Qlucore Omics Explorer 3.2. Differentially expressed genes were determined using an F-test across all time points (omnibus ANOVA). Multiple testing correction was performed using the Benjamini-Hochberg algorithms with a false discovery rate (FDR) of 1%. For correlations between mRNA and protein responses, Pearson correlation coefficients were computed on fold changes of mRNA and protein abundances at the respective time points relative to t0. Pathway analyses were performed using Ingenuity Pathway Analysis (IPA, QIAgen). Global gene expression data from control and AF/PLL-treated PHH were used to extract miRNA expression levels that were further normalized to t0. Corresponding fold-change values for upregulated miRNAs were interpreted in the microRNA Target Filter of IPA to find corresponding downregulated mRNA targets from whole transcriptome data of the same samples. Resulting gene lists were submitted to the WebGestalt online resource for KEGG pathway analysis[25].

Extended methods are available in the Supporting Information online.

Results

Transcriptomic changes occur in two distinct phases of molecular remodeling during hepatocyte dedifferentiation.

To decode the changes in transcriptional profiles during dedifferentiation of PHH we assessed gene expression dynamics using whole transcriptome approaches in which coding as well as non-coding RNA transcripts were analyzed with high temporal resolution (n=3-5 livers per time point). In total, we identified 4,042 transcripts that were significantly differentially expressed during the first 24 hours of dedifferentiation after multiple testing correction (FDR=0.01, Figure 1A). Importantly, we detected two distinct phases of transcriptomic changes: an early response (from 30 minutes until 4 hours) and a late response (between 16 and 24 hours) that were characterized by changes in two distinctively different sets of genes (Figure 1B).

Pathway analyses of differentially expressed transcripts over time revealed significant modulations of cytokine and signal transduction pathways such as IL-1 and PKA signaling as well as PPARα/RXRα transcriptional responses already after 30 minutes followed by major restructuring of metabolic pathways evidenced by changes in oxidative phosphorylation and mitochondrial dysfunction (Figure 1C and Supporting Table 2). The earliest responses were detected in genes involved in innate immunity, whereas expression changes in genes involved in absorption, distribution, metabolism and excretion (ADME) of drugs as well as cell adhesion were found at later phases (Supporting Figure 1). Furthermore, alterations in EIF2 signaling and protein ubiquitination pathways suggest modulations of protein turnover. Significant changes at later stages of hepatic dedifferentiation included major metabolic pathways such as the TCA cycle, ketogenesis, the urea cycle and fatty acid metabolism.

To probe whether transcriptomic alterations were faithful markers of phenotypic changes during dedifferentiation, we performed whole-proteome analyses. Overall, we detected less expressed proteins than coding transcripts (2,356 proteins vs. 20,667 transcripts) most likely due to the low expression levels of many proteins such as transcription factors as well as the relatively lower sensitivity of mass spectrometry-based methods. To assess the agreement between responses on mRNA and protein level, we correlated transcriptomic and proteomic changes. Interestingly, while correlations were poor after 4 hours (r=0.16), they improved substantially after 24 hours (r=0.72; Figure 1D). Notably, abundances of most CYP proteins, such as CYP2A6, CYP2B6, CYP2C19 and CYP2D6 were only moderately affected after 24 hours of dedifferentiation in agreement with long half-lives of this class of proteins[11,26], whereas their corresponding transcript levels were strongly reduced. The overall proteomic changes followed transcriptomic profiles with the exception of fatty acid β-oxidation, which was first detected at the proteomic levels (Figure 1C and Supporting Table 3). We concluded that changes in transcriptomic signatures translate into phenotypic changes during early hepatocyte dedifferentiation and are thus suitable markers to study underlying regulatory processes.

When we categorized differentially expressed transcripts into protein-coding genes, miRNAs, lncRNAs, snoRNAs and ribosomal genes (rRNAs and ribosomal proteins, we observed that changes in these ncRNA classes peaked at 4 hours, whereas an impact on coding genes was predominantly observed later (Figure 2). Furthermore, whereas protein-coding genes showed a tendency to be rather downregulated during dedifferentiation (52.4% downregulated), non-coding genes were predominantly upregulated (Figure 2C-F). Interestingly, among the different classes of ncRNAs, the

dynamics and direction of regulation of lncRNAs Figure 2D) more closely resembled the temporal and directional profiles of coding genes (Figure 2B), possibly, at least in part, because of a positive correlation between the transcription of lncRNA and their proximal protein-coding genes[27].

miRNA levels are substantially reduced in primary hepatocytes upon small molecule inhibition of the miRNA machinery.

Based on the dynamics and direction of transcriptomic changes, we hypothesized that modulations of the ncRNAome could be causal for alterations observed in protein-coding genes and thus for the loss of the hepatocyte phenotype. To test this hypothesis, we focused specifically on miRNAs since miRNA biogenesis and action is mediated by only few genes that constitute the miRNA processing machinery. We inhibited the miRNA pathway at two distinct nodes using two well-characterized, chemically distinct compounds, acriflavine (AF) and poly-L-lysine (PLL). While PLL is reported to inhibit the association of pre-miRNAs to Dicer, AF impairs RISC by inhibition of miRNA binding to AGO family proteins[28]. No toxicity of AF and PLL was detected at any of the concentrations tested after 4 hours ($p>0.15$ for all, Supporting Figure 2). After 24 hours, PLL affected viability only minimally even at high concentrations (viability PLL_{hi} = 86%±4%), whereas AF was more toxic with increasing concentrations. Consequently, we chose to focus on samples treated with low AF (viability AF_{low} = 71%±4%) and high PLL concentrations, respectively.

First, we assessed the effect of AF and PLL on expression levels of a set of specific miRNAs with important roles in liver function (Figure 3A). Hepatic miRNAs miR-

103 and miR-107 that regulate insulin sensitivity[29] were upregulated during dedifferentiation, an effect that was inhibited by PLL and to a lesser extent by AF. Similarly, levels of the pro-proliferative miRNAs miR-21, miR-122 and miR-221, which target the cell cycle inhibitors *BTG2*, *HMOX1* and *CDKN1B*[30-32], respectively, were rapidly increased, consistent with an initiation of the hepatic regeneration program. No significant changes were detected in the anti-proliferative miR-22 and miR-26a ($p>0.05$ for both miRs after 4 and 24h compared to t0, data not shown). Yet, levels of the anti-proliferative miRNA miR-33a, a direct inhibitor of *CDK6* and *CCND1*[33] were massively increased during dedifferentiation. Importantly, PLL and AF generally reduced the burst of miRNA expression observed in untreated samples, indicating that small molecule inhibition of the miRNA machinery might be an effective means to reduce overall miRNA levels.

Next, we assessed the effect of AF and PLL on miRNA levels on a global scale and detected a decrease in overall miRNA expression levels (Figure 3B). While after 4h, 12% (AF) and 7% (PLL) of all expressed miRNA were downregulated >1.5-fold, after 24h 32% (AF) and 43% were downregulated upon AF and PLL treatment, respectively compared to control at the same time point (Figure 3C), thus confirming that inhibition of the miRNA machinery results in substantially reduced levels of mature miRNAs in the cell within the time frame studied.

Inhibition of the miRNA machinery delays the loss of hepatic differentiation markers

To address the impact of miRNA inhibition during hepatic dedifferentiation, we assessed whether AF- and PLL-mediated miRNA inhibition impacts hepatocyte dedifferentiation kinetics. We analyzed the changes in expression levels of 110 genes, including phase I and phase II enzymes, transporters, nuclear receptors and other genes with importance for hepatic functionality (Figure 4). We found that expression of these hepatic genes decreased rapidly in untreated hepatocytes with some genes being downregulated by up to 97% (*SLCO1B1* and *SLCO1B3*) after only 4 hours of culture (Figure 4B). Importantly, inhibition of the miRNA machinery largely mitigated the loss of marker gene expression (Figure 4 and qPCR validations in Supporting Figure 3). Consistent with the downregulation of hepatic genes during dedifferentiation, expression levels of the vast majority of these genes were found to be increased compared to untreated controls at the same time point (Figure 4C). We noticed that effect sizes of our treatments differed substantially between genes, as expression levels of *CYP3A4* and *HNF4A* increased only to a limited extent, whereas the effect on *CYP2C8* and *CYP2C9* was much more prominent (Figure 4A and Supporting Figure 3).

To substantiate the conceptual role of miRNAs in dedifferentiation, we specifically inhibited miR-103, a miRNA that was strongly affected by AF and PLL treatment, using specific antagomiRs (Supporting Figure 3). We found that expression of its *bona fide* target gene *CYP2C8*[34] was significantly increased, thus providing evidence that candidate miRNA inhibition can contribute to a delay of dedifferentiation when only considering its particular target transcript subset.

We conclude that while the extent and kinetics to which hepatic marker genes are regulated by miRNAs can differ, inhibition of the miRNA machinery has overall profound effects on dedifferentiation at the molecular level.

miRNA inhibition reduces overall hepatocyte dedifferentiation.

To assess the impact of miRNA inhibition during dedifferentiation beyond alterations of expression patterns in hepatic markers, we correlated expression fold-changes for each gene after 4 hours and 24 hours of dedifferentiation in control with PLL- and AF-treated samples (Figure 5). The slope of the regression lines indicates the extent of dedifferentiation for a given treatment and time-point relative to control. After only 4 hours, transcriptomic signatures were significantly different between control and inhibitor-treated samples ($p<0.0001$, F-test comparing control and AF/PLL regression lines). In inhibitor-treated samples, expression levels were generally less affected compared to control (95% CI of regression slopes: ($a_{PLL,4h}$) = 0.7-0.71; 95% CI($a_{AF,4h}$) = 0.76-0.76; Figure 5A,B), an effect became even more pronounced over time as transcriptomic fingerprints more closely resembled samples prior to dedifferentiation than dedifferentiated control samples after 24 hours of culture (95% CI($a_{PLL,24h}$) = 0.24-0.25; 95% CI($a_{AF,24h}$) = 0.27-0.28; Figure 5C,D). Furthermore, when considering only genes that were found to be differentially expressed during dedifferentiation (see Fig. 1), we found that changes in their gene expression signatures, indicative of dedifferentiation were drastically reduced (Supporting Figure 5).

While transcriptomes of treated and control samples correlated significantly ($p<0.0001$ for both AF and PLL, F-test), the expression levels of some individual genes differed drastically. When considering only those genes whose expression levels were increased >10-fold in miRNA-inhibitor treated samples, we found them to be enriched in both AF- and PLL-treated samples in acute phase response signaling, the complement system, FXR/RXR and PXR/RXR activation, thus suggesting prolongation of immune response signaling and a positive effect on liver specific functionality (see Supporting Table 4). Genes that were downregulated >10-fold in inhibitor-treated samples were enriched in adherence junction, actin cytoskeleton and ILK signaling. Again, very similar results were obtained using both AF and PLL.

Interestingly, transcriptomic changes in response to inhibition of the miRNA machinery were mostly symmetrically distributed in up- and downregulated genes compared to control (Supporting Fig. 6). Nevertheless, the fraction of genes that were downregulated less in treated compared to control samples was enriched especially after 24 hours (red columns, Supporting Fig. 6).

We then analyzed the effects of AF and PLL specifically on the miRNAome and associated pathways by matching upregulated miRNAs with their predicted target transcripts within the same experiment (Table 2). In control samples, metabolic pathways, protein processing in the endoplasmic reticulum and fatty acid metabolism were most significantly affected. Importantly, significantly fewer genes of the respective networks were targeted in AF- and PLL-treated samples in agreement with overall reduced dedifferentiation.

Combined, our data indicate that inhibition of the miRNA machinery results in drastic changes in the hepatic dedifferentiation program, strongly reducing the loss of hepatic markers and mitigating alterations in adherence junction signaling and cytoskeletal remodeling, suggesting a key role for miRNAs in driving the underlying molecular processes.

Discussion

Hepatocytes are very dynamic cells *in vivo* that can rapidly switch between non-dividing states during liver homeostasis and dividing states upon liver injury. During this process, they undergo a wide range of molecular changes including alterations in marker gene expression, indicating that they can transiently dedifferentiate into more progenitor-like states[8,9]. Following proliferation, cells redifferentiate and thus replenish the pool of mature hepatocytes within the regenerating organ[9]. Mechanistic understanding of how hepatocytes can alter their differentiation states can give valuable information for the generation of hepatocytes from stem cells.

Dedifferentiation also occurs *in vitro* as rapid loss of marker gene expression and hepatic functionality are observed when PHH are placed in 2D culture. This loss of liver functions is detrimental in drug discovery and assessment programs where new chemical entities are tested e.g. for metabolism, toxicity, drug interactions and induction, as results form the basis for the development of clinical programs.

In this study we demonstrate that gradual changes in genes related to immunity and energy balance occurred during the first 4 hours of culture, followed by later changes in major metabolic pathways. Notably, the response at the proteomic level mostly overlapped and followed transcriptomic changes with respect to pathway enrichments, indicating that transcriptomic changes are overall faithful markers of phenotypic alterations in the early phases of hepatocyte dedifferentiation. Interestingly, transcriptomic and proteomic responses correlated only very weakly after 4 hours (r=0.16), probably at least in part due to the widespread transcriptomic remodeling, which has not been fully translated to the level of protein abundances. In contrast, correlations after 24 hours are significantly higher (r=0.72) and similar to values reported for murine liver (r=0.6 for mRNA vs. protein copy numbers)[35].

When expression changes were resolved by gene class, the highest number of differentially expressed genes was detected after 4 hours of culture. Notably, the upregulation of ribosomal genes was paralleled by an activation of mTOR and EIF2 signaling, which primes cells for increased mRNA translation, foreshadowing a massive remodeling of cellular functionality and phenotypes[36,37]. Furthermore, the canonical function of snoRNAs is the 2'-O-methylation and pseudouridylation of ribosomal RNAs, again hinting at an overall translational activation[18].

To functionally test the role of miRNAs as potential drivers of the dedifferentiation program, we used AF and PLL. PLL inhibits Dicer-dependent processing of pre-miRNA molecules into mature miRNAs, manifesting in reduced miRNA levels[28], which is consistent the global reduction in miRNA levels (Figure 3). In contrast, AF

blocks the binding of mature miRNA molecules to AGO family proteins and hence does not directly impact miRNA levels[28]. Yet, previous studies showed that unbound miRNAs are less stable than miRNAs bound to RISC[38], which could explain the variability in expression levels of the different miRNAs. The extent of reduction in expression upon inhibitor treatment varied substantially between different miRNAs. While miR-33a levels were below detection limit upon PLL treatment already after 4 hours, levels of miR-21 were not affected, suggesting vastly different miRNA half-lives. This finding contrasts previous studies that reported miRNAs half-lives to range from hours to days, indicating that the inherent stability might differ miRNA species but also between primary cells during major remodeling processes and cell cultures in static conditions[39]. Notably, the slow kinetics of genetic or siRNA-based approaches for miRNA-inhibition combined with long half-lives of protein components of the miRNA machinery[40] render such tools inadequate to inhibit miRNA action within the timeframe in which molecular changes occur. Therefore, small molecule inhibition presents currently the only viable option to perturb rapidly enough.

While hepatocytes proliferate *in vivo* after partial hepatectomy, dedifferentiation *in vitro* is not paralleled by hepatic proliferation. Even when cells are stimulated with growth factors, proliferation quickly ceases and cells enter cell cycle arrest[41]. This discrepancy between proliferative responses *in vivo* and *in vitro* correlates with the differences in response of miR-33 whose expression is reduced during liver regeneration, relieving inhibition of CDK6 and Cyclin D1 expression thereby supporting entry of cells into mitosis. In contrast, miR-33a expression is strongly increased *in vitro* (Figure 3A), hampering cell cycle entry. Thus, inhibition of miR-

33a might present a novel approach to stimulate proliferation of primary hepatocytes *in vitro*.

Importantly, analyses of expression kinetics of 110 hepatic genes revealed that their downregulation was mostly reduced with both miRNA inhibitors, yet to varying extents (Figure 4 and Supporting Fig. 3). While the decrease in e.g. *CYP2A6*, *CYP2C8*, *CYP2C9*, *CYP2D6* and *SLC22A1* expression was strongly reduced, only minor elevations of transcript levels were observed for *CYP3A4*. Our results are in agreement with previous experimental findings showing that *CYP2C8* (miR-103/107) and *CYP2C9* (miR-128) are strongly regulated by miRNAs[34,42]. Furthermore, a recent screen for miRNAs as modulators of *CYP3A4* activity revealed only minor inhibition[43] consistent with the low but significant increase in *CYP3A4* transcript levels observed here. To validate these findings, we inhibited miR-103 using a specific antagomiR and found that its *bona fide* target gene *CYP2C8* was upregulated accordingly during dedifferentiation (Supporting Figure 4). These experimental indications about the extent to which miRNAs regulate ADME gene expression further incentivizes their therapeutic targeting and warrants investigations of the impact of miRNAs on the disposition of co-administered drugs[44]. Yet, further studies are required to quantify the recruitment of specific miRNAs to the RISC, as bound miRNAs might be more faithful reporters for regulatory load during liver regeneration than overall transcriptional levels[45].

Combined, our data indicate that (i) an upregulation of a multitude of miRNAs precedes the loss of hepatic marker gene expression and (ii) that this dedifferentiation

is diminished when the miRNA pathway is either generally inhibited or when candidate miRNAs are blocked in a targeted approach. Importantly though, not all hepatic markers that we analyzed responded to miRNA inhibition with similar magnitude indicating that also other regulatory mechanisms such as short transcript half-lives potentially contribute to a rapid downregulation of transcript levels.

When we correlated expression fold-changes in control and miRNA inhibitor-treated samples, we found that the ameliorating effect on dedifferentiation increased after 24 hours, possibly due to indirect effects such as the regulation of core transcription factors (Figure 5). Most considerably "rescued" pathways by miRNA inhibition were complement system and cytokine signaling, cytoskeleton, cell adhesion, and hepatic expression programs such as PXR/RXR activation (Figure 5C,D), thus mirroring deregulated pathways during dedifferentiation and indicating an overall improvement of hepatic phenotype. While the data presented here indicates that miRNA changes constitute an integral part of the hepatic dedifferentiation program, the upstream cues that trigger the initiation of dedifferentiation, remain to be elucidated. To this end, a variety of stimuli have been suggested, including harsh hepatocyte isolation conditions as such, serum depletion, alterations in cell-ECM or cell-cell contacts and exposure to non-physiological stiffness of culture substratum[46,47]. However, as hepatocytes retain their functionality when cultured as 3D spheroids in serum-free conditions[48], perturbations of cell-ECM or cell-cell contacts and exposure to non-physiological stiffness of culture substratum appear to be most likely causes.

The data presented here might exemplify a more general biological principle of dynamic cellular adaptation. miRNAs might serve as the tool of choice for the cell to quickly degrade particular mRNA and/or inhibit their translation, especially those with a long half-life, and thus facilitate expeditious remodeling of the transcriptomic inventory when rapid adjustments are needed in response to changes in environment or specific signaling cues as seen in other contexts, such as T-cell activation[49]. Furthermore, as miRNAs can have pleiotropic targets thereby diversifying an incoming stimulus into a wide range of downstream targets, thus serving as a molecular signal amplifier.

In conclusion, our results indicate a novel role for miRNAs in hepatic processes and implicate them as important drivers of hepatic dedifferentiation. As such, these findings are of importance for understanding mechanisms of stem cell differentiation into hepatocytes as well as for liver regeneration, during which similar dedifferentiation processes might occur *in vivo*. Furthermore, the data presented here might highlight a more wide-spread miRNA-mediated dynamic control of transcriptional profiles that warrants further investigations.

Acknowledgements

We thank Drs. Roz Jenkins and Joanne Walsh for support with proteomic analyses.

Supporting Information

Additional Supporting information can be found online.

Figure 1: Profiling of early events in hepatic dedifferentiation on transcriptomic and proteomic level reveals overall molecular rearrangements. (**A**) Heatmap visualization of mean-centered, sigma-normalized expression data of differentially expressed genes during the first 24 hours of hepatocyte dedifferentiation (n=4,042, FDR=0.01) reveals an early response in which expression changes accumulate progressively during the first 4 hours and (ii) a later response in which a different set of genes was affected. Numbers in the colored circles indicate the respective hepatocyte donor (Table 1). (**B**) Principle component analysis of differentially expressed genes shown in **A** resulted in the identification of two orthogonal components for early and late transcriptomic changes. (**C**) Pathway analysis of differentially expressed genes revealed the temporal order of events. Pathways identified as differentially regulated in at least 2 consecutive time points with $p<0.05$ on transcriptomic (blue) and proteomic level (red) are shown. (**D**) Scatter plots showing the correlations between mean changes in mRNA levels and the corresponding average changes in protein abundances after 4 hours and 24 hours in culture. The mean of 3 donors is plotted.

Figure 2: Early changes in non-coding RNAs precede rearrangements of the coding transcriptome during hepatocyte dedifferentiation. (**A**) Stacked column

plot visualizing the number of up- and downregulated genes at each time point compared to t0. Coding genes are shown in blue, non-coding genes in grey. Small pie charts associated to each column indicate the relative fractions of differentially expressed non-coding RNAs at the respective time point categorized by gene class. Note that the highest number of differentially expressed genes was found after 4 hours and was dominated by upregulated non-coding RNAs. (**B**-**E**) Stacked column plots showing the profiles of transcriptomic changes resolved by gene class and up- and downregulation (dark and light hue, respectively) into protein-coding genes (**B**), miRNAs (**C**), lncRNAs (**D**), snoRNAs (**E**) and ribosomal genes (**F**). y-axis indicates differentially expressed genes. While protein-coding genes were up- and downregulated, non-coding genes had a strong bias for upregulation especially at early time points.

Figure 3: miRNA expression during hepatocyte dedifferentiation can be inhibited using small molecule inhibitors. The miRNA machinery was inhibited using acriflavine (AF) and poly-L-lysine (PLL). All expression levels were normalized to expression prior to dedifferentiation (t0). (**A**) Expression of all six miRNAs shown were elevated during dedifferentiation in control samples (blue). This increase in miRNA levels was mostly inhibited dose-dependently by AF (red) and PLL treatment (green). Inhibitor-treated samples were compared with the corresponding controls at the same time point using heteroscedastic two-tailed t-tests. Error bars indicate s.e. * indicates $p<0.05$, ** indicates $p<0.01$. n.d. indicates expression below detection limit. N=6 experiments for controls and 3 for inhibitor-treated samples (**B, C**) Transcriptomic assessment of miRNA levels upon AF- and PLL-treatment. (**B**) Heatmap displaying expression changes of all detected miRNAs.

(**C**) Column plot showing the fraction of expressed miRNAs that were downregulated more than 1.5-fold compared to control at the same time point. In total n=210 different miRNAs were robustly detected in all samples.

Figure 4: Inhibition of the miRNA machinery ameliorates changes in hepatic genes during hepatic dedifferentiation. (**A**) Heatmap visualization of mean-centered, sigma-normalized expression data of 110 genes with importance for hepatic functionality. Note that while many hepatic genes are rapidly lost in control samples, treatment with AF and PLL overall decreases this effect. (**B**, **C**) Dot plot representations visualizing the change of expression of the same 110 hepatic genes compared to timepoint 0 (**B**) or to the corresponding control at the same time point (**C**). Notably, *CYP2A6*, a specialized indicator of hepatic differentiation[11], is upregulated 8- and 26-fold in AF and PLL-treated samples after 24h, respectively. FC = fold change.

Figure 5: Evaluation of overall transcriptomic changes in response to miRNA inhibitors reveals drastically reduced dedifferentiation. Scatter log-plots of transcriptomic changes (n=61,933 gene products) in control samples versus changes in AF- or PLL-treated cultures after 4 h (**A**-**B**) and 24 h (**C**-**D**). Red and green dots highlight genes that are up- or downregulated >10-fold under treatment, respectively. These form the basis for the analysis of most affected pathways shown in red and green inlet boxes. Solid red lines indicate complete dedifferentiation in control samples (slope a=1). Dashed red lines indicate computed regression lines. Note that regression line slopes (a_{inh}) can be interpreted as the extent of dedifferentiation and

were <1 for all time points and treatments, indicating decreased overall dedifferentiation at the systems level. Values for r indicate Pearson correlation coefficients.

References

1 Michalopoulos, G.K. Liver regeneration. *Journal of Cellular Physiology* **213**, 286-300 (2007).

2 Fausto, N., Campbell, J.S. & Riehle, K.J. Liver regeneration. *Hepatology* **43**, S45-S53 (2006).

3 Yovchev, M. I. *et al.* Identification of adult hepatic progenitor cells capable of repopulating injured rat liver. *Hepatology* **47**, 636-647 (2007).

4 Kordes, C. & Häussinger, D. Hepatic stem cell niches. *Journal of Clinical Investigation* **123**, 1874-1880 (2013).

5 Evarts, R.P., Nagy, P., Marsden, E. & Thorgeirsson, S.S. A precursor-product relationship exists between oval cells and hepatocytes in rat liver. *Carcinogenesis* **8**, 1737-1740 (1987).

6 Schaub, J.R., Malato, Y., Gormond, C. & Willenbring, H. Evidence against a Stem Cell Origin of New Hepatocytes in a Common Mouse Model of Chronic Liver Injury. *Cell Reports* **8**, 933-939 (2014).

7 **Yanger, K., Knigin, D**. *et al.* Adult Hepatocytes Are Generated by Self-Duplication Rather than Stem Cell Differentiation. *Cell Stem Cell* **15**, 340-349, (2014).

8 **Yanger, K., Zong, Y**. *et al.* Robust cellular reprogramming occurs spontaneously during liver regeneration. *Genes & Development* **27**, 719-724, (2013).

9 Tarlow, B.D. *et al.* Bipotential Adult Liver Progenitors Are Derived from Chronically Injured Mature Hepatocytes. *Stem Cell* **15**, 605-618 (2014).

10 Chen, Y., Wong, P.P., Sjeklocha, L., Steer, C.J. & Sahin, M.B. Mature hepatocytes exhibit unexpected plasticity by direct dedifferentiation into liver progenitor cells in culture. *Hepatology* **55**, 563-574 (2012).

11 Rowe, C. *et al.* Proteome-wide analyses of human hepatocytes during differentiation and dedifferentiation. *Hepatology* **58**, 799-809 (2013).

12 Baker, T.K. *et al.* Temporal Gene Expression Analysis of Monolayer Cultured Rat Hepatocytes. *Chemical Research in Toxicology* **14**, 1218-1231 (2001).

13 Cech, T.R. & Steitz, J.A. The Noncoding RNA Revolution— Trashing Old Rules to Forge New Ones. *Cell* **157**, 77-94 (2014).

14 Wilczynska, A. & Bushell, M. The complexity of miRNA-mediated repression. *Cell Death and Differentiation* **22**, 22-33 (2015).

15 Gamazon, E.R. *et al.* A genome-wide integrative study of microRNAs in human liver. *BMC Genomics* **14**, 395 (2013).

16 Kim, N. *et al.* Expression profiles of miRNAs in human embryonic stem cells during hepatocyte differentiation. *Hepatology Research* **41**, 170-183 (2011).

17 Clouet d'Orval, B., Bortolin, M.L., Gaspin, C. & Bachellerie, J.P. Box C/D RNA guides for the ribose methylation of archaeal tRNAs. The tRNATrp intron guides the formation of two ribose-methylated nucleosides in the mature tRNATrp. *Nucleic Acids Research* **29**, 4518-4529 (2001).

18 Decatur, W.A. & Fournier, M.J. rRNA modifications and ribosome function. *Trends in Biochemical Sciences* **27**, 344-351 (2002).

19 Taft, R.J. *et al.* Small RNAs derived from snoRNAs. *RNA* **15**, 1233-1240 (2009).

20 **Kishore, S., Kanna, A**. *et al.* The snoRNA MBII-52 (SNORD 115) is processed into smaller RNAs and regulates alternative splicing. *Human Molecular Genetics* **19**, 1153-1164 (2010).

21 **Ender, C., Krek, A.** *et al.* A Human snoRNA with MicroRNA-Like Functions. *Molecular Cell* **32**, 519-528 (2008).

22 **Sharma, E., Sterne-Weiler, T**., O'Hanlon, D. & Blencowe, B.J. Global Mapping of Human RNA-RNA Interactions. *Molecular Cell* **62**, 618-626, (2016).

23 Kung, J.T., Colognori, D. & Lee, J.T. Long Noncoding RNAs: Past, Present, and Future. *Genetics* **193**, 651-669 (2013).

24 Strom, S.C. *et al.* Use of human hepatocytes to study P450 gene induction. *Methods in Enzymology* **272**, 388-401 (1996).

25 Wang, J., Duncan, D., Shi, Z. & Zhang, B. WEB-based GEne SeT AnaLysis Toolkit (WebGestalt): update 2013. *Nucleic Acids Research* **41**, W77-W83 (2013).

26 Yang, J. *et al.* Cytochrome p450 turnover: regulation of synthesis and degradation, methods for determining rates, and implications for the prediction of drug interactions. *Current Drug Metabolism* **9**, 384-394 (2008).

27 **Andersson, R., Gebhard, C**. *et al.* An atlas of active enhancers across human cell types and tissues. *Nature* **507**, 455-461, (2014).

28 Watashi, K., Yeung, M.L., Starost, M.F., Hosmane, R.S. & Jeang, K.T. Identification of Small Molecules That Suppress MicroRNA Function and Reverse Tumorigenesis. *Journal of Biological Chemistry* **285**, 24707-24716 (2010).

29 Trajkovski, M. *et al.* MicroRNAs 103 and 107 regulate insulin sensitivity. *Nature* **474**, 649-653 (2011).

30 Liu, M. *et al.* Regulation of the cell cycle gene, BTG2, by miR-21 in human laryngeal carcinoma. *Cell Research* **19**, 828-837 (2009).

31 John, K. *et al.* MicroRNAs play a role in spontaneous recovery from acute liver failure. *Hepatology* **60**, 1346-1355 (2014).

32 Fornari, F. *et al.* MiR-221 controls CDKN1C/p57 and CDKN1B/p27 expression in human hepatocellular carcinoma. *Oncogene* **27**, 5651-5661 (2008).

33 **Cirera-Salinas, D., Pauta, M**. *et al.* Mir-33 regulates cell proliferation and cell cycle progression. *Cell Cycle* **11**, 922-933, (2012).

34 **Zhang, S.Y., Surapureddi, S**., Coulter, S., Ferguson, S.S. & Goldstein, J.A. Human CYP2C8 Is Post-Transcriptionally Regulated by MicroRNAs 103 and 107 in Human Liver. *Molecular Pharmacology* **82**, 529-540, (2012).

35 Azimifar, S.B., Nagaraj, N., Cox, J. & Mann, M. Cell-Type-Resolved Quantitative Proteomics of Murine Liver. *Cell Metabolism* **20**, 1076-1087 (2014).

36 Xiao, L. & Grove, A. Coordination of Ribosomal Protein and Ribosomal RNA Gene Expression in Response to TOR Signaling. *Current Genomics* **10**, 198-205 (2009).

37 Kimball, S.R. Eukaryotic initiation factor eIF2. *The International Journal of Biochemistry & Cell Biology* **31**, 25-29 (1999).

38 Diederichs, S. & Haber, D.A. Dual Role for Argonautes in MicroRNA Processing and Posttranscriptional Regulation of MicroRNA Expression. *Cell* **131**, 1097-1108 (2007).

39 **Gantier, M.P., McCoy, C.E.** *et al.* Analysis of microRNA turnover in mammalian cells following Dicer1 ablation. *Nucleic Acids Research* **39**, 5692-5703 (2011).

40 **Olejniczak, S.H., La Rocca, G.,** Gruber, J. J. & Thompson, C. B. Long-lived microRNA-Argonaute complexes in quiescent cells can be activated to regulate mitogenic responses. *PNAS* **110**, 157-162 (2013).

41 Runge, D.M. *et al.* Epidermal growth factor- and hepatocyte growth factor-receptor activity in serum-free cultures of human hepatocytes. *Journal of Hepatology* **30**, 265-274 (1999).

42 Yu, D. *et al.* Suppression of CYP2C9 by MicroRNA hsa-miR-128-3p in Human Liver Cells and Association with Hepatocellular Carcinoma. *Scientific Reports* **5**, 8534-8539 (2015).

43 **Wei, Z., Jiang, S**. *et al.* The Effect of microRNAs in the Regulation of Human CYP3A4: a Systematic Study using a Mathematical Model. *Scientific Reports* **4**, 1-7 (2014).

44 Li, Z. & Rana, T.M. Therapeutic targeting of microRNAs: current status and future challenges. *Nature Genetics* **13**, 622-638 (2014).

45 **Schug, J., McKenna, L.B**. *et al.* Dynamic recruitment of microRNAs to their mRNA targets in the regenerating liver. *BMC Genomics* **14**, 264 (2013).

46 Elaut, G. *et al.* Molecular mechanisms underlying the dedifferentiation process of isolated hepatocytes and their cultures. *Current Drug Metabolism* **7**, 629-660 (2006).

47 Godoy, P. *et al.* Extracellular matrix modulates sensitivity of hepatocytes to fibroblastoid dedifferentiation and transforming growth factor β-induced apoptosis. *Hepatology* **49**, 2031-2043 (2009).

48 **Bell, C.C., Hendriks, D.F., Moro, S.M.** *et al.* Characterization of primary human hepatocyte spheroids as a model system for drug-induced liver injury, liver function and disease. *Scientific Reports*, 1-13 (2016).

49 Bronevetsky, Y. *et al.* T cell activation induces proteasomal degradation of Argonaute and rapid remodeling of the microRNA repertoire. *Journal of Experimental Medicine* **210**, 417-432 (2013).

HEP-16-0352.R2

Title: Massive rearrangements of cellular miRNA signatures are key drivers of hepatocyte dedifferentiation

Volker M. Lauschke[1]*, Sabine U. Vorrink[1], Sabrina M. Moro[1], Fatemah Reyazee[1], Åsa Nordling[1], Delilah F. Hendriks[1], Catherine C. Bell[1], Rowena Sison-Young[2], B. Kevin Park[2], Christopher E. Goldring[2], Ewa Ellis[3], Inger Johansson[1], Souren Mkrtchian[1], Tommy B. Andersson[1,4] and Magnus Ingelman-Sundberg[1]

[1] Section of Pharmacogenetics, Department of Physiology and Pharmacology, Karolinska Institutet, SE-17177 Stockholm, Sweden.

[2] MRC Centre for Drug Safety Science, Department of Molecular and Clinical Pharmacology, Sherrington Buildings, Ashton Street, University of Liverpool, UK.

[3] Department of Clinical Science, Intervention and Technology, Karolinska University Hospital Huddinge, Karolinska Institutet, Stockholm, Sweden

[4] Cardiovascular and Metabolic Diseases Innovative Medicines, DMPK, AstraZeneca R&D, SE-431 83, Mölndal, Sweden

* To whom correspondence should be addressed

Volker M. Lauschke, Karolinska Institutet, Department of Physiology and Pharmacology, Section of Pharmacogenetics, Nanna Svartz Väg 2, 17177 Stockholm, Sweden, Phone: +46 8524 87711, Fax: +46 8337 327, E-mail: volker.lauschke@ki.se

Sabine U. Vorrink, Karolinska Institutet, Department of Physiology and Pharmacology, Section of Pharmacogenetics, Nanna Svartz Väg 2, 17177 Stockholm, Sweden, Phone: +46 8524 87762, Fax: +46 8337 327, E-mail: sabine.vorrink@ki.se

Sabrina M. L. Moro, Karolinska Institutet, Department of Physiology and Pharmacology, Section of Pharmacogenetics, Nanna Svartz Väg 2, 17177 Stockholm, Sweden, Phone: +46 8524 87762, Fax: +46 8337 327, E-mail: sabrina.ml.moro@gmail.com

Fatemah Reyazee, Karolinska Institutet, Department of Physiology and Pharmacology, Section of Pharmacogenetics, Nanna Svartz Väg 2, 17177 Stockholm, Sweden, Phone: +46 8524 87711, Fax: +46 8337 327, E-mail: fatemah.rezayee@hotmail.se

Åsa Nordling, Karolinska Institutet, Department of Physiology and Pharmacology, Section of Pharmacogenetics, Nanna Svartz Väg 2, 17177 Stockholm, Sweden, Phone: +46 8524 87762, Fax: +46 8337 327, E-mail: asa.nordling@ki.se

Delilah F. G. Hendriks, Karolinska Institutet, Department of Physiology and Pharmacology, Section of Pharmacogenetics, Nanna Svartz Väg 2, 17177 Stockholm, Sweden, Phone: +46 8524 87711, Fax: +46 8337 327, E-mail: delilah.hendriks@ki.se

Catherine Bell, Karolinska Institutet, Department of Physiology and Pharmacology, Section of Pharmacogenetics, Nanna Svartz Väg 2, 17177 Stockholm, Sweden, Phone: +46 8524 87711, Fax: +46 8337 327, E-mail: catherine.bell@ki.se

Rowena Sison-Young, MRC Centre for Drug Safety Science, Department of Molecular and Clinical Pharmacology, Sherrington Buildings, Ashton Street, University of Liverpool, Liverpool, L69 3GE, UK. Email: rowena.sison-young@liverpool.ac.uk

B. Kevin Park, MRC Centre for Drug Safety Science, Department of Molecular and Clinical Pharmacology, Sherrington Buildings, Ashton Street, University of Liverpool, Liverpool, L69 3GE, UK. Email: B.K.Park@liverpool.ac.uk

Christopher E.P. Goldring, MRC Centre for Drug Safety Science, Department of Molecular and Clinical Pharmacology, Sherrington Buildings, Ashton Street, University of Liverpool, Liverpool, L69 3GE, UK. Email: chrissy@liv.ac.uk

Ewa Ellis, Department of Clinical Science, Intervention and Technology, Karolinska University Hospital Huddinge, Karolinska Institutet, Stockholm, Sweden E mail: ewa.ellis@ki.se

Inger Johansson, Karolinska Institutet, Department of Physiology and Pharmacology, Section of Pharmacogenetics, Nanna Svartz Väg 2, 17177 Stockholm, Sweden, Phone: +46 8524 87762, Fax: +46 8337 327, E-mail: inger.johansson@ki.se

Souren Mkrtchian, Karolinska Institutet, Department of Physiology and Pharmacology, Section of Pharmacogenetics, Nanna Svartz Väg 2, 17177 Stockholm, Sweden, Phone: +46 8524 87762, Fax: +46 8337 327, E-mail: souren.mkrtchian@ki.se

Tommy B. Andersson, AstraZeneca, R&D, Cardiovascular and Metabolic Diseases, Innovative Medicines and Early Development Biotech Unit, Pepparedsleden 1, 43183 Mölndal, Sweden, Phone: +46 317761534, Fax: +46 317763786, Email: tommy.b.andersson@astrazeneca.com

Magnus Ingelman-Sundberg, Karolinska Institutet, Department of Physiology and Pharmacology, Section of Pharmacogenetics, Nanna Svartz Väg 2, 17177 Stockholm, Sweden, Phone: +46 8524 877 35, Fax: +46 8337 327, E-mail: magnus.ingelman-sundberg@ki.se

Corresponding author: Volker M. Lauschke, Karolinska Institutet, Department of Physiology and Pharmacology, Section of Pharmacogenetics, Nanna Svartz Väg 2, 17177 Stockholm, Sweden, Phone: +46 8524 87711, Fax: +46 8337 327, E-mail: volker.lauschke@ki.se

List of Abbreviations: PHH: primary human hepatocytes; CYP: cytochrome P450; ncRNA: non-coding RNA; miRNA: micro RNA; snoRNA: small nucleolar RNA; lncRNA: long non-coding RNA; RISC: RNA-induced silencing complex; ADME: absorption, distribution, metabolism and excretion; AF: acriflavine; PLL: poly-L-lysine.

Keywords: miRNA, transcriptomics, primary human hepatocytes, cytochrome P450, drug metabolism

Conflict of interest: V.M.L. and M.I.-S. are founders and owners of HepaPredict AB.

Financial support: This work was supported by grants from AstraZeneca, The Swedish Research Council and by the European Community under the Innovative

Medicine Initiative project MIP-DILI [grant agreement number 115336]. V.M.L. was supported by a MarieCurie IEF fellowship for career development in the context of the European FP7 framework program and by a grant from the Eva och Oscar Ahrèns Stiftelse.

Electronic Word Count: 5994 words

Abstract

Hepatocytes are dynamic cells that upon injury can alternate between non-dividing differentiated and dedifferentiated proliferating states *in vivo*. However, in 2D cultures primary human hepatocytes rapidly dedifferentiate resulting in the loss of hepatic functions which significantly limits their usefulness as *in vitro* model of liver biology, liver diseases as well as drug metabolism and toxicity. Thus, understanding the underlying mechanisms and stalling of the dedifferentiation process would be highly beneficial to establish more accurate and relevant long-term *in vitro* hepatocyte models. Here, we present comprehensive analyses of whole proteome and transcriptome dynamics during the initiation of dedifferentiation during the first 24 hours of culture. We report that early major rearrangements of the non-coding transcriptome, hallmarked by increased expression of snoRNAs, lncRNAs, miRNAs, and ribosomal genes, precede most changes in coding genes during dedifferentiation of primary human hepatocytes and we speculated that these modulations could drive the hepatic dedifferentiation process. To functionally test this hypothesis, we globally inhibited the miRNA machinery using two established chemically-distinct compounds, acriflavine and poly-L-lysine. These inhibition experiments resulted in a significantly impaired miRNA response and, most importantly, in a pronounced reduction in the downregulation of hepatic genes with importance for liver function. Thus, we provide strong evidence for the importance of ncRNAs, in particular miRNAs, in hepatic dedifferentiation, which can aid the development of more efficient differentiation protocols for stem cell-derived hepatocytes and broaden our understanding of the dynamic properties of hepatocytes with respect to liver regeneration.

Conclusion: miRNAs are important drivers of hepatic dedifferentiation and our results provide valuable information regarding the mechanisms behind liver regeneration and possibilities to inhibit dedifferentiation *in vitro*.

Introduction

Upon liver injury, hepatic cells proliferate and rapidly regenerate large parts of the damaged organ *in vivo*[1]. Different mechanisms of liver regeneration have been described in different injury models. Under most injuries, such as partial hepatectomy, the liver regenerates by self-duplication of hepatocytes[2]. Yet, when hepatocyte proliferation is compromised, the formation of duct-like "oval cells" with a mixed mesenchymal and epithelial expression signature has been observed[3]. These progenitor cells are assumed to originate from the terminal branches of the intrahepatic biliary system[4] and seminal work demonstrated that these cells can give rise to hepatocytes[5]. Yet, recent studies in mouse models of chronic liver insults indicated that new hepatocytes originated from pre-existing hepatocytes rather than from distinguished non-parenchymal stem-cell populations[6,7]. One explanation for this ostensible discrepancy might be the capacity of hepatocytes to undergo reversible ductal metaplasia, which opens the possibility that hepatocyte-derived progenitor cells expressing biliary markers are mistaken for progenitor cells of biliary origin[8,9].

~~Cell-labeling experiments indicate that the new hepatocytes originate from mature hepatocytes rather than from distinguished stem-cell populations[2,3]. This hepatocyte expansion is assumed to involve transient dedifferentiation followed by proliferation and redifferentiation, which demonstrates an astonishing plasticity of liver cells regarding their differentiation states[4,5].~~

In vitro in 2D monolayer cultures, primary human hepatocytes (PHH) rapidly lose their phenotype and dedifferentiate into fetal-like progenitor states with drastically reduced- liver-specific functionality, which hampers their usefulness for studies of liver biology, liver disease, drug metabolism and toxicity[10,11]. Most importantly, PHH

rapidly lose expression of important liver-specific genes, such as cytochrome P450 (CYP) enzymes, phase 2 enzymes and transporters[12]. Therefore, decipherment and eventual inhibition of the dedifferentiation process could allow for more accurate and relevant long-term *in vitro* hepatocyte models. Furthermore, mechanistic understanding of the dedifferentiation process can guide the development of more efficient differentiation protocols for stem cell-derived hepatocytes. Until now however, the molecular cues that initiate the dedifferentiation process and its mediators that render hepatocytes capable to respond so rapidly to a changing cellular environment have remained elusive.

Changes in transcript levels can be modulated by non-coding (nc)RNA species such as micro (mi)RNAs, small nucleolar (sno)RNAs, and long non-coding (lnc)RNAs[13]. miRNAs are short single-stranded RNAs that associate with the RNA-induced silencing complex (RISC) by binding to AGO proteins, downregulating protein output of complementary transcripts by translational inhibition or transcript degradation[14]. An *in silico* study using 79 human livers showed that levels of 275 miRNAs ~~were inversely~~ correlated inversely with expression patterns of their putative hepatic target genes[15]. Furthermore, analyses of miRNA expression during the differentiation of stem cells to hepatocyte-like cells implicated dozens of miRNAs in these developmental programs[16]. Yet, miRNA dynamics during hepatocyte dedifferentiation remain to be elucidated. Combined, these data suggest that miRNAs are of paramount importance for liver function and hepatic differentiation and merit detailed investigation.

snoRNAs guide modifications of other ncRNA species such as ribosomal RNAs, thereby contributing to the remodeling of the cell's translational capabilities[17,18]. Furthermore, many snoRNAs harbor sno-derived (sd)RNAs that are commonly conserved across species from vertebrates to plants[19]. Interestingly, some sdRNAs have been shown to impact alternative splicing and are implicated in disease (e.g. SNORD115 in Prader-Willi syndrome[20]), while others control levels of target mRNAs[21,22].

lncRNAs are a rapidly growing class of ncRNAs that can influence protein output by regulating transcription of nearby or distal genes, impacting splicing, RNA stability or translation, as well as acting as miRNA decoys (see [23] and references therein). lncRNAs are difficult to study *en bloc* because (i) they cannot be predicted solely on their sequence and (ii) the functionality and molecular mode of action of most lncRNA family members remains poorly understood.

While mounting evidence indicates important roles for ncRNAs in hepatic dedifferentiation, their dynamics and functional effects have not been quantitatively assessed with high temporal resolution. Therefore, we here thoroughly characterized changes in coding and non-coding transcriptomes during dedifferentiation of PHH using unsupervised whole transcriptome analyses. We detected massive alterations of ncRNA signatures that preceded changes in coding transcripts during later stages of dedifferentiation. In order to investigate whether these ncRNA modulations could drive the dedifferentiation process, we established a miRNA inhibition assay using two chemically-distinct inhibitors that interfere with different nodes of the miRNA-

processing pathway. We found that miRNA inhibition significantly reduced the early miRNA response and the loss of hepatic marker genes. Moreover, whole-transcriptome analyses revealed that gene expression changes during dedifferentiation in inhibitor-treated samples were globally reduced, thus providing strong evidence for the importance of ncRNAs, in particular miRNAs, in hepatic dedifferentiation.

Materials and Methods

Hepatocytes cultures

Fresh hepatocytes obtained from patients subject to liver resections at Huddinge University Hospital, Stockholm, Sweden were used for the dedifferentiation experiments (Table 1). The hepatocytes obtained from patient livers were isolated as previously described[24]. Use of liver specimens was approved by the Ethics Committee at Karolinska Institutet and written informed consent was obtained from all donors of liver material. Hepatocytes were seeded into plates coated with 5 µg/cm^2 Rat Tail Collagen Type I (Corning) in culture medium (Williams E medium supplemented with 2mM L-glutamine, 100 units/ml penicillin, 100 µg/ml streptomycin, 10 µg/ml insulin, 5.5 µg/ml transferrin, 6.7 ng/ml sodium selenite, 100nM dexamethasone) with 10% FBS. After two hours of attachment, the medium was replaced with serum-free culture medium. Time point 0 (t0) is defined as immediately before plating. The other time points denote time passed since plating.

miRNA inhibition experiments

Cryopreserved hepatocytes were thawed according to the supplier's protocol (BioreclamationIVT) and cultured as above. Cells were treated with 2 (low), 10 (medium) or 30 µM (high) AF or 1 (low), 5 (medium) or 15 µM (high) PLL as indicated.

Statistical analyses

Unsupervised hierarchical clustering and principal component analysis of genes was performed in Qlucore Omics Explorer 3.2. Differentially expressed genes were determined using an F-test across all time points (omnibus ANOVA). Multiple testing correction was performed using the Benjamini-Hochberg algorithms with a false discovery rate (FDR) of 1%. For correlations between mRNA and protein responses, Pearson correlation coefficients were computed on fold changes of mRNA and protein abundances at the respective time points relative to t0. Pathway analyses were performed using Ingenuity Pathway Analysis (IPA, QIAgen). Global gene expression data from control and AF/PLL-treated PHH were used to extract miRNA expression levels that were further normalized to t0. Corresponding fold-change values for upregulated miRNAs were interpreted in the microRNA Target Filter of IPA to find corresponding downregulated mRNA targets from whole transcriptome data of the same samples. Resulting gene lists were submitted to the WebGestalt online resource for KEGG pathway analysis[25].

Extended methods are available in the Supporting Information online.

Results

Transcriptomic changes occur in two distinct phases of molecular remodeling during hepatocyte dedifferentiation.

To decode the changes in transcriptional profiles during dedifferentiation of PHH we ~~analyzed~~ assessed gene expression dynamics using whole transcriptome approaches in which coding as well as non-coding RNA transcripts were analyzed with high temporal resolution (n=3-5 livers per time point). In total, we identified 4,042 transcripts that were significantly differentially expressed during the first 24 hours of dedifferentiation after multiple testing correction (FDR=0.01, Figure 1A). Importantly, we detected two distinct phases of transcriptomic changes: an early response (from 30 minutes until 4 hours) and a late response (between 16 and 24 hours) that were characterized by changes in two distinctively different sets of genes (Figure 1B).

Pathway analyses of differentially expressed transcripts over time revealed significant modulations of cytokine and signal transduction pathways such as IL-1 and PKA signaling as well as PPARα/RXRα transcriptional responses already after 30 minutes followed by major restructuring of metabolic pathways evidenced by changes in oxidative phosphorylation and mitochondrial dysfunction (Figure 1C and Supporting Table 2). The earliest responses were detected in genes involved in innate immunity, whereas expression changes in genes involved in absorption, distribution, metabolism and excretion (ADME) of drugs as well as cell adhesion were found at later phases (Supporting Figure 1). Furthermore, alterations in EIF2 signaling and protein

ubiquitination pathways suggest modulations of protein turnover. Significant changes at later stages of hepatic dedifferentiation included major metabolic pathways such as the TCA cycle, ketogenesis, the urea cycle and fatty acid metabolism.

To probe whether transcriptomic alterations were faithful markers of phenotypic changes during dedifferentiation, we performed whole-proteome analyses. Overall, we detected ~~significantly~~ less expressed proteins than coding transcripts (2,356 proteins vs. 20,667 transcripts) most likely due to the low expression levels of many proteins such as transcription factors as well as the relatively lower sensitivity of mass spectrometry-based methods. To assess the agreement between responses on mRNA and protein level, we correlated transcriptomic and proteomic changes. Interestingly, while correlations were poor after 4 hours (r=0.16), they improved substantially after 24 hours (r=0.72; Figure 1D). Notably, abundances of most CYP proteins, such as CYP2A6, CYP2B6, CYP2C19 and CYP2D6 were only moderately affected after 24 hours of dedifferentiation in agreement with long half-lives of this class of proteins[11,26], whereas their corresponding transcript levels were strongly reduced. The overall proteomic changes followed transcriptomic profiles with the exception of fatty acid β-oxidation, which was first detected at the proteomic levels (Figure 1C and Supporting Table 3). We concluded that changes in transcriptomic signatures translate into phenotypic changes during early hepatocyte dedifferentiation and are thus suitable markers to study underlying regulatory processes.

When we categorized differentially expressed transcripts into protein-coding genes, miRNAs, lncRNAs, snoRNAs and ribosomal genes (rRNAs and ribosomal proteins,

we observed that changes in these ncRNA classes peaked at 4 hours, whereas an impact on coding genes was predominantly observed later (Figure 2). Furthermore, whereas protein-coding genes showed a tendency to be rather downregulated during dedifferentiation (52.4% downregulated), non-coding genes were predominantly upregulated (Figure 2C-F). Interestingly, among the different classes of ncRNAs, the dynamics and direction of regulation of lncRNAs Figure 2D) more closely resembled the temporal and directional profiles of coding genes (Figure 2B), possibly, at least in part, because of a positive correlation between the transcription of lncRNA and their proximal protein-coding genes[27].

miRNA levels are substantially reduced in primary hepatocytes upon small molecule inhibition of the miRNA machinery.

Based on the dynamics and direction of transcriptomic changes, we hypothesized that modulations of the ncRNAome could be causal for alterations observed in protein-coding genes and thus for the loss of the hepatocyte phenotype. To test this hypothesis, we focused specifically on miRNAs since miRNA biogenesis and action is mediated by only few genes that constitute the miRNA processing machinery. We inhibited the miRNA pathway at two distinct nodes using two well-characterized, chemically distinct compounds, acriflavine (AF) and poly-L-lysine (PLL). While PLL is reported to inhibit the association of pre-miRNAs to Dicer, AF impairs RISC by inhibition of miRNA binding to AGO family proteins[28]. No toxicity of AF and PLL was detected at any of the concentrations tested after 4 hours ($p>0.15$ for all, Supporting Figure 2). After 24 hours, PLL affected viability only minimally even at high concentrations (viability PLL_{hi} = 86%±4%), whereas AF was more toxic with

increasing concentrations. Consequently, we chose to focus on samples treated with low AF (viability AF_{low} = 71%±4%) and high PLL concentrations, respectively.

First, we assessed the effect of AF and PLL on expression levels of a set of specific miRNAs with important roles in liver function (Figure 3A). Hepatic miRNAs miR-103 and miR-107 that regulate insulin sensitivity[29] were upregulated during dedifferentiation, an effect that was inhibited by PLL and to a lesser extent by AF. Similarly, levels of the pro-proliferative miRNAs miR-21, miR-122 and miR-221, which target the cell cycle inhibitors *BTG2*, *HMOX1* and *CDKN1B*[30-32], respectively, were rapidly increased, consistent with an initiation of the hepatic regeneration program. No significant changes were detected in the anti-proliferative miR-22 and miR-26a ($p>0.05$ for both miRs after 4 and 24h compared to t0, data not shown). Yet, levels of the anti-proliferative miRNA miR-33a, a direct inhibitor of *CDK6* and *CCND1*[33] were massively increased during dedifferentiation. Importantly, PLL and AF generally reduced the burst of miRNA expression observed in untreated samples, indicating that small molecule inhibition of the miRNA machinery might be an effective means to reduce overall miRNA levels.

Next, we assessed the effect of AF and PLL on miRNA levels on a global scale and detected a decrease in overall miRNA expression levels (Figure 3B). While after 4h, 12% (AF) and 7% (PLL) of all expressed miRNA were downregulated >1.5-fold, after 24h 32% (AF) and 43% were downregulated upon AF and PLL treatment, respectively compared to control at the same time point (Figure 3C), thus confirming

that inhibition of the miRNA machinery results in substantially reduced levels of mature miRNAs in the cell within the time frame studied.

Inhibition of the miRNA machinery delays the loss of hepatic differentiation markers

To address the impact of miRNA inhibition during hepatic dedifferentiation, we assessed whether AF- and PLL-mediated miRNA inhibition impacts hepatocyte dedifferentiation kinetics. We analyzed the changes in expression levels of 110 genes, including phase I and phase II enzymes, transporters, nuclear receptors and other genes with importance for hepatic functionality (Figure 4). We found that expression of these hepatic genes decreased rapidly in untreated hepatocytes with some genes being downregulated by up to 97% (*SLCO1B1* and *SLCO1B3*) after only 4 hours of culture (Figure 4B). Importantly, inhibition of the miRNA machinery largely mitigated the loss of marker gene expression (Figure 4 and qPCR validations in Supporting Figure 3). Consistent with the downregulation of hepatic genes during dedifferentiation, expression levels of the vast majority of these genes were found to be increased compared to untreated controls at the same time point (Figure 4C). We noticed that effect sizes of our treatments differed substantially between genes, as expression levels of *CYP3A4* and *HNF4A* increased only to a limited extent, whereas the effect on *CYP2C8* and *CYP2C9* was much more prominent (Figure 4A and Supporting Figure 3).

To substantiate the conceptual role of miRNAs in dedifferentiation, we specifically inhibited miR-103, a miRNA that was strongly affected by AF and PLL treatment,

using specific antagomiRs (Supporting Figure 3). We found that expression of its *bona fide* target gene *CYP2C8*[34] was significantly increased, thus providing evidence that candidate miRNA inhibition can contribute to a delay of dedifferentiation when only considering its particular target transcript subset.

We conclude that while the extent and kinetics to which hepatic marker genes are regulated by miRNAs can differ, inhibition of the miRNA machinery has overall profound effects on dedifferentiation at the molecular level.

miRNA inhibition reduces overall hepatocyte dedifferentiation.

To assess the impact of miRNA inhibition during dedifferentiation beyond alterations of expression patterns in hepatic markers, we correlated expression fold-changes for each gene after 4 hours and 24 hours of dedifferentiation in control with PLL- and AF-treated samples (Figure 5). The slope of the regression lines indicates the extent of dedifferentiation for a given treatment and time-point relative to control. After only 4 hours, transcriptomic signatures were significantly different between control and inhibitor-treated samples ($p<0.0001$, F-test comparing control and AF/PLL regression lines). In inhibitor-treated samples, expression levels were generally less affected compared to control (95% CI of regression slopes: ($a_{PLL,4h}$) = 0.7-0.71; 95% CI($a_{AF,4h}$) = 0.76-0.76; Figure 5A,B), an effect became even more pronounced over time as transcriptomic fingerprints more closely resembled samples prior to dedifferentiation than dedifferentiated control samples after 24 hours of culture (95% CI($a_{PLL,24h}$) =

0.24-0.25; 95% CI($a_{AF,24h}$) = 0.27-0.28; Figure 5C,D). Furthermore, when considering only genes that were found to be differentially expressed during dedifferentiation (see Fig. 1), we found that changes in their gene expression signatures, indicative of dedifferentiation were drastically reduced (Supporting Figure 5).

While transcriptomes of treated and control samples correlated significantly ($p<0.0001$ for both AF and PLL, F-test), the expression levels of some individual genes differed drastically. When considering only those genes whose expression levels were increased >10-fold in miRNA-inhibitor treated samples, we found them to be enriched in both AF- and PLL-treated samples in acute phase response signaling, the complement system, FXR/RXR and PXR/RXR activation, thus suggesting prolongation of immune response signaling and a positive effect on liver specific functionality (see Supporting Table 4). Genes that were downregulated >10-fold in inhibitor-treated samples were , among others, enriched in adherence junction, signaling, the actin cytoskeleton and ILK signaling. Again, very similar results were obtained using both AF and PLL.

Interestingly, transcriptomic changes in response to inhibition of the miRNA machinery were mostly symmetrically distributed in up- and downregulated genes compared to control (Supporting Fig. 6). Nevertheless, the fraction of genes that were downregulated less in treated compared to control samples was enriched especially after 24 hours (red columns, Supporting Fig. 6).

We then analyzed the effects of AF and PLL specifically on the miRNAome and associated pathways by matching upregulated miRNAs with their predicted target transcripts within the same experiment (Table 2). In control samples, metabolic pathways, protein processing in the endoplasmic reticulum and fatty acid metabolism were most significantly affected. Importantly, significantly fewer genes of the respective networks were targeted in AF- and PLL-treated samples in agreement with overall reduced dedifferentiation.

Combined, our data indicate that inhibition of the miRNA machinery results in drastic changes in the hepatic dedifferentiation program, strongly reducing the loss of hepatic markers and mitigating alterations in adherence junction signaling and cytoskeletal remodeling, suggesting a key role for miRNAs in driving the underlying molecular processes.

Discussion

Hepatocytes are very dynamic cells *in vivo* that can rapidly switch between non-dividing states during liver homeostasis and dividing states upon liver injury. During this process, they undergo a wide range of molecular changes including alterations in marker gene expression, indicating that they can transiently dedifferentiate into more progenitor-like states[8,9]. Following proliferation, cells redifferentiate and thus replenish the pool of mature hepatocytes within the regenerating organ[9]. Mechanistic understanding of how hepatocytes can alter their differentiation states can give

valuable information for the generation of hepatocytes from stem cells. Dedifferentiation also occurs *in vitro* as rapid loss of marker gene expression and hepatic functionality are observed when PHH are placed in 2D culture. This loss of liver functions is detrimental in drug discovery and assessment programs where new chemical entities are tested e.g. for metabolism, toxicity, drug interactions and induction, as results ~~are considered a reliable~~form the basis for the development of clinical programs ~~and the use of the potential drug compounds~~[34].

In this study~~,~~ we demonstrate that gradual changes in genes related to immunity and energy balance occurred during the first 4 hours of culture, followed by later changes in major metabolic pathways. Notably, the response at the proteomic level mostly overlapped and followed transcriptomic changes with respect to pathway enrichments, indicating that transcriptomic changes are overall faithful markers of phenotypic alterations in the early phases of hepatocyte dedifferentiation. Interestingly, transcriptomic and proteomic responses correlated only very weakly after 4 hours (r=0.16), probably at least in part due to the widespread transcriptomic remodeling, which has not been fully translated to the level of protein abundances. In contrast, correlations after 24 hours are significantly higher (r=0.72) and similar to values reported for murine liver (r=0.6 for mRNA vs. protein copy numbers)[35].

When expression changes were resolved by gene class, the highest number of differentially expressed genes was detected after 4 hours of culture. Notably, the upregulation of ribosomal genes was paralleled by an activation of mTOR and EIF2 signaling, which primes cells for increased mRNA translation, foreshadowing a

massive remodeling of cellular functionality and phenotypes[36,37]. Furthermore, the canonical function of snoRNAs is the 2'-O-methylation and pseudouridylation of ribosomal RNAs, again hinting at an overall translational activation[18].

To functionally test the role of ~~non-coding~~mi-RNAs as potential drivers of the dedifferentiation program, we used AF and PLL. PLL inhibits Dicer-dependent ~~and thus the~~ processing of pre-miRNA molecules into mature ~~single stranded~~ miRNAs, manifesting in reduced miRNA levels[28], which is consistent the global reduction in miRNA levels (Figure 3). In contrast, AF blocks the binding of mature miRNA molecules to AGO family proteins and hence does not directly impact miRNA levels[28]. Yet, previous studies showed that unbound miRNAs are less stable than miRNAs bound to RISC[38], which could explain the variability in expression levels of the different miRNAs. The extent of reduction in expression upon inhibitor treatment varied substantially between different miRNAs. While miR-33a levels were below detection limit upon PLL treatment already after 4 hours, levels of miR-21 were not affected, suggesting vastly different miRNA half-lives. This finding ~~is interesting as~~contrasts previous studies that reported ~~that~~ miRNAs ~~are very stable with~~ half-lives ~~ranging~~ to range from hours to days, indicating that the inherent stability might differ miRNA species but also between primary cells during major remodeling processes and cell cultures in static ~~culture~~ conditions[39]. Notably, the slow kinetics of genetic or siRNA-based approaches for miRNA-inhibition combined with long half-lives of protein components of the miRNA machinery[40] render such tools inadequate to inhibit miRNA action within the timeframe in which molecular changes occur. Therefore,

small molecule inhibition presents currently the only viable option to perturb rapidly enough.

While hepatocytes proliferate *in vivo* after partial hepatectomy, dedifferentiation *in vitro* is not paralleled by hepatic proliferation. Even when cells are stimulated with growth factors, proliferation quickly ceases and cells enter cell cycle arrest[41]. This discrepancy between proliferative responses *in vivo* and *in vitro* correlates with the differences in response of miR-33 ~~as expression of this miRNA~~whose expression is reduced during liver regeneration, relieving inhibition of CDK6 and Cyclin D1 expression thereby supporting entry of cells into mitosis. In contrast,~~,~~ ~~whereas *in vitro*~~ miR-33a expression is strongly increased ~~*in vitro* as indicated above~~(Figure 3A), hampering cell cycle entry. Thus, inhibition of miR-33a might present a novel approach to stimulate proliferation of primary hepatocytes *in vitro*.

Formatted: Font: Italic

Importantly, analyses of expression kinetics of 110 hepatic genes revealed that their downregulation was mostly reduced with both miRNA inhibitors, yet to varying extents (Figure 4 and Supporting Fig. 3). While the decrease in e.g. *CYP2A6*, *CYP2C8*, *CYP2C9*, *CYP2D6* and *SLC22A1* expression was strongly reduced, only minor elevations of transcript levels were observed for *CYP3A4*. Our results are in agreement with previous experimental findings ~~experimentally~~ showing that *CYP2C8* (miR-103/107) and *CYP2C9* (miR-128) are strongly regulated by miRNAs[34,42]. Furthermore, a recent screen for miRNAs as modulators of *CYP3A4* activity revealed only minor inhibition[43] consistent with the low but significant increase in *CYP3A4* transcript levels observed here. To validate these findings, we inhibited miR-103

using a specific antagomiR and found that its *bona fide* target gene *CYP2C8* was upregulated accordingly during dedifferentiation (Supporting Figure 4). These experimental indications about the extent to which miRNAs regulate ADME gene expression further incentivizes their therapeutic targeting and warrants investigations of the impact of miRNAs on the disposition of co-administered drugs[44]. Yet, further studies are required to quantify the recruitment of specific miRNAs to the RISC, as bound miRNAs might be more faithful reporters for regulatory load during liver regeneration than overall transcriptional levels[45]~~Yet, further studies will be needed to quantify the extent of regulation exerted by specific miRNAs as recruitment of mature miRNAs to the RISC rather than overall transcriptional levels might be more faithful reporters for miRNA regulatory load during liver regeneration[4445]~~.

Combined, our data indicate that (i) an upregulation of a multitude of miRNAs precedes the loss of hepatic marker gene expression and (ii) that this dedifferentiation is diminished when the miRNA pathway is either generally inhibited or when candidate miRNAs are blocked in a targeted approach. Importantly though, not all hepatic markers that we analyzed responded to miRNA inhibition with similar magnitude indicating that also other regulatory mechanisms such as short transcript half-lives potentially contribute to a rapid downregulation of transcript levels.

When we correlated expression fold-changes in control and miRNA inhibitor-treated samples, we found that the ameliorating effect on dedifferentiation increased after 24 hours, possibly due to indirect effects such as the regulation of core transcription factors (Figure 5). ~~The pathways that were m~~Most ~~strongly~~ considerably "rescued"

pathways by miRNA inhibition were complement system and cytokine signaling, cytoskeleton, cell adhesion, and hepatic expression programs such as PXR/RXR activation (Figure 5C,D), thus mirroring deregulated pathways during dedifferentiation and indicating an overall improvement of hepatic phenotype. While the data presented here indicates that miRNA changes constitute an integral part of the hepatic dedifferentiation program, the upstream cues that trigger the initiation of dedifferentiation, remain to be elucidated. To this end, a variety of stimuli have been suggested, including ~~the~~ harsh hepatocyte isolation ~~procedure~~ conditions as such, serum depletion, alterations in ~~ECM interfaces~~ cell-ECM or cell-cell contacts and exposure to non-physiological stiffness of culture substratum[46,47]. However, as hepatocytes retain their functionality when cultured as 3D spheroids in serum-free conditions[48] ~~However, based on results that functionality is retained when isolated hepatocytes are cultured as 3D spheroids in serum-free conditions~~[47], ~~the alterations in ECM interfaces~~perturbations of cell-ECM or cell-cell contacts and exposure to non-physiological stiffness of culture substratum appear to be ~~the~~ most likely ~~explanations~~causes.

The data presented here might exemplify a more general biological principle of dynamic cellular adaptation. miRNAs might serve as the tool of choice for the cell to quickly degrade particular mRNA and/or inhibit their translation, especially those with a long half-life, and thus facilitate expeditious remodeling of the transcriptomic inventory when rapid adjustments are needed in response to changes in environment or specific signaling cues as seen in other contexts, such as T-cell activation[49]. Furthermore, as miRNAs can have pleiotropic targets thereby diversifying an

incoming stimulus into a wide range of downstream targets, thus serving as a molecular signal amplifier.

In conclusion, our results indicate a novel role for miRNAs in hepatic processes and implicate them as important drivers of hepatic dedifferentiation. As such, these findings are of importance for understanding mechanisms of stem cell differentiation into hepatocytes as well as for liver regeneration, during which similar dedifferentiation processes might occur *in vivo*. Furthermore, the data presented here might highlight a more wide-spread miRNA-mediated dynamic control of transcriptional profiles that warrants further investigations.

Acknowledgements

We thank Drs. Roz Jenkins and Joanne Walsh for support ~~in the~~with proteomic analyses.

Supporting Information

Additional Supporting information can be found online.

Figure 1: Profiling of early events in hepatic dedifferentiation on transcriptomic and proteomic level reveals overall molecular rearrangements. (**A**) Heatmap visualization of mean-centered, sigma-normalized expression data of differentially expressed genes during the first 24 hours of hepatocyte dedifferentiation (n=4,042, FDR=0.01) reveals an early response in which expression changes accumulate progressively during the first 4 hours and (ii) a later response in which a different set of genes was affected. Numbers in the colored circles indicate the respective hepatocyte donor (Table 1). (**B**) Principle component analysis of differentially expressed genes shown in **A** resulted in the identification of two orthogonal components for early and late transcriptomic changes. (**C**) Pathway analysis of differentially expressed genes revealed thea temporal order of events. Pathways identified as differentially regulated in at least 2 consecutive time points with $p<0.05$ on transcriptomic ~~level~~ (blue) and proteomic level (red) are shown ~~in blue and on proteomic level in red~~. ~~Only differentially regulated pathways that were identified in at least 2 consecutive time points with $p<0.05$ are shown.~~ (**D**) Scatter plots showing the correlations between mean changes in mRNA levels and the corresponding average changes in protein abundances after 4 hours and 24 hours in culture. The mean of 3 donors is plotted.

Figure 2: Early changes in non-coding RNAs precede rearrangements of the coding transcriptome during hepatocyte dedifferentiation. (**A**) Stacked column plot visualizing the number of up- and downregulated genes at each time point compared to t0. Coding genes are shown in blue, non-coding genes in grey. Small pie charts associated to each column indicate the relative fractions of differentially expressed non-coding RNAs at the respective time point categorized by gene class.

Note that the highest number of differentially expressed genes was found after 4 hours and was dominated by upregulated non-coding RNAs. (**B-E**) Stacked column plots showing the profiles of transcriptomic changes resolved by gene class and up- and downregulation (dark and light hue, respectively) into protein-coding genes (**B**), miRNAs (**C**), lncRNAs (**D**), snoRNAs (**E**) and ribosomal genes (**F**). y-axis indicates differentially expressed genes. While protein-coding genes were up- and downregulated, non-coding genes had a strong bias for upregulation especially at early time points.

Figure 3: miRNA expression during hepatocyte dedifferentiation can be inhibited using small molecule inhibitors. The miRNA machinery was inhibited using acriflavine (AF) and poly-L-lysine (PLL). All expression levels were normalized to expression prior to dedifferentiation (t0). (**A**) Expression of all six miRNAs shown were elevated during dedifferentiation in control samples (blue). This increase in miRNA levels was mostly inhibited dose-dependently by AF (red) and PLL treatment (green). Inhibitor-treated samples were compared with the corresponding controls at the same time point using heteroscedastic two-tailed t-tests. Error bars indicate s.e. * indicates $p<0.05$, ** indicates $p<0.01$. n.d. indicates expression below detection limit. N=6 experiments for controls and 3 for inhibitor-treated samples (**B, C**) Transcriptomic assessment of miRNA levels upon AF- and PLL-treatment. (**B**) Heatmap displaying expression changes of all detected miRNAs. (**C**) Column plot showing the fraction of expressed miRNAs that were downregulated more than 1.5-fold compared to control at the same time point. In total n=210 different miRNAs were robustly detected in all samples.

Figure 4: Inhibition of the miRNA machinery ameliorates changes in hepatic genes during hepatic dedifferentiation. (**A**) Heatmap visualization of mean-centered, sigma-normalized expression data of 110 genes with importance for hepatic functionality. Note that while many hepatic genes are rapidly lost in control samples, treatment with AF and PLL overall decreases this effect. (**B**, **C**) Dot plot representations visualizing the change of expression of the same 110 hepatic genes compared to timepoint 0 (**B**) or to the corresponding control at the same time point (**C**). Notably, *CYP2A6*, a specialized indicator of hepatic differentiation[11], is upregulated 8- and 26-fold in AF and PLL-treated samples after 24h, respectively. FC = fold change.

Figure 5: Evaluation of overall transcriptomic changes in response to miRNA inhibitors reveals drastically reduced dedifferentiation. Scatter log-plots of transcriptomic changes (n=61,933 gene products) in control samples versus changes in AF- or PLL-treated cultures after 4 h (**A**-**B**) and 24 h (**C**-**D**). Red and green dots highlight genes that are up- or downregulated >10-fold under treatment, respectively. These form the basis for the analysis of most affected pathways shown in red and green inlet boxes. Solid red lines indicate complete dedifferentiation in control samples (slope a=1). Dashed red lines indicate computed regression lines. Note that regression line slopes (a_{inh}) can be interpreted as the extent of dedifferentiation and were <1 for all time points and treatments, indicating decreased overall dedifferentiation at the systems level. Values for r indicate Pearson correlation coefficients.

References

1 Michalopoulos, G.K. Liver regeneration. *Journal of Cellular Physiology* **213**, 286-300 (2007).

2 Fausto, N., Campbell, J.S. & Riehle, K.J. Liver regeneration. *Hepatology* **43**, S45-S53 (2006).

3 Yovchev, M. I. *et al.* Identification of adult hepatic progenitor cells capable of repopulating injured rat liver. *Hepatology* **47**, 636-647 (2007).

4 Kordes, C. & Häussinger, D. Hepatic stem cell niches. *Journal of Clinical Investigation* **123**, 1874-1880 (2013).

5 Evarts, R.P., Nagy, P., Marsden, E. & Thorgeirsson, S.S. A precursor-product relationship exists between oval cells and hepatocytes in rat liver. *Carcinogenesis* **8**, 1737-1740 (1987).

6 Schaub, J.R., Malato, Y., Gormond, C. & Willenbring, H. Evidence against a Stem Cell Origin of New Hepatocytes in a Common Mouse Model of Chronic Liver Injury. *Cell Reports* **8**, 933-939 (2014).

7 **Yanger, K., Knigin, D**. *et al.* Adult Hepatocytes Are Generated by Self-Duplication Rather than Stem Cell Differentiation. *Cell Stem Cell* **15**, 340-349, (2014).

8 **Yanger, K., Zong, Y**. *et al.* Robust cellular reprogramming occurs spontaneously during liver regeneration. *Genes & Development* **27**, 719-724, (2013).

9 Tarlow, B.D. *et al.* Bipotential Adult Liver Progenitors Are Derived from Chronically Injured Mature Hepatocytes. *Stem Cell* **15**, 605-618 (2014).

10 Chen, Y., Wong, P.P., Sjeklocha, L., Steer, C.J. & Sahin, M.B. Mature hepatocytes exhibit unexpected plasticity by direct dedifferentiation into liver progenitor cells in culture. *Hepatology* **55**, 563-574 (2012).

11 Rowe, C. *et al.* Proteome-wide analyses of human hepatocytes during differentiation and dedifferentiation. *Hepatology* **58**, 799-809 (2013).

12 Baker, T.K. *et al.* Temporal Gene Expression Analysis of Monolayer Cultured Rat Hepatocytes. *Chemical Research in Toxicology* **14**, 1218-1231 (2001).

13 Cech, T.R. & Steitz, J.A. The Noncoding RNA Revolution— Trashing Old Rules to Forge New Ones. *Cell* **157**, 77-94 (2014).

14 Wilczynska, A. & Bushell, M. The complexity of miRNA-mediated repression. *Cell Death and Differentiation* **22**, 22-33 (2015).

15 Gamazon, E.R. *et al.* A genome-wide integrative study of microRNAs in human liver. *BMC Genomics* **14**, 395 (2013).

16 Kim, N. *et al.* Expression profiles of miRNAs in human embryonic stem cells during hepatocyte differentiation. *Hepatology Research* **41**, 170-183 (2011).

17 Clouet d'Orval, B., Bortolin, M.L., Gaspin, C. & Bachellerie, J.P. Box C/D RNA guides for the ribose methylation of archaeal tRNAs. The tRNATrp intron guides the formation of two ribose-methylated nucleosides in the mature tRNATrp. *Nucleic Acids Research* **29**, 4518-4529 (2001).

18 Decatur, W.A. & Fournier, M.J. rRNA modifications and ribosome function. *Trends in Biochemical Sciences* **27**, 344-351 (2002).

19 Taft, R.J. *et al.* Small RNAs derived from snoRNAs. *RNA* **15**, 1233-1240 (2009).

20 **Kishore, S., Kanna, A**. *et al.* The snoRNA MBII-52 (SNORD 115) is processed into smaller RNAs and regulates alternative splicing. *Human Molecular Genetics* **19**, 1153-1164 (2010).

21 **Ender, C., Krek, A.** *et al.* A Human snoRNA with MicroRNA-Like Functions. *Molecular Cell* **32**, 519-528 (2008).

22 **Sharma, E., Sterne-Weiler, T**., O'Hanlon, D. & Blencowe, B.J. Global Mapping of Human RNA-RNA Interactions. *Molecular Cell* **62**, 618-626, (2016).

23 Kung, J.T., Colognori, D. & Lee, J.T. Long Noncoding RNAs: Past, Present, and Future. *Genetics* **193**, 651-669 (2013).

24 Strom, S.C. *et al.* Use of human hepatocytes to study P450 gene induction. *Methods in Enzymology* **272**, 388-401 (1996).

25 Wang, J., Duncan, D., Shi, Z. & Zhang, B. WEB-based GEne SeT AnaLysis Toolkit (WebGestalt): update 2013. *Nucleic Acids Research* **41**, W77-W83 (2013).

26 Yang, J. *et al.* Cytochrome p450 turnover: regulation of synthesis and degradation, methods for determining rates, and implications for the prediction of drug interactions. *Current Drug Metabolism* **9**, 384-394 (2008).

27 **Andersson, R., Gebhard, C**. *et al.* An atlas of active enhancers across human cell types and tissues. *Nature* **507**, 455-461, (2014).

28 Watashi, K., Yeung, M.L., Starost, M.F., Hosmane, R.S. & Jeang, K.T. Identification of Small Molecules That Suppress MicroRNA Function and Reverse Tumorigenesis. *Journal of Biological Chemistry* **285**, 24707-24716 (2010).

29 Trajkovski, M. *et al.* MicroRNAs 103 and 107 regulate insulin sensitivity. *Nature* **474**, 649-653 (2011).

30 Liu, M. *et al.* Regulation of the cell cycle gene, BTG2, by miR-21 in human laryngeal carcinoma. *Cell Research* **19**, 828-837 (2009).

31 John, K. *et al.* MicroRNAs play a role in spontaneous recovery from acute liver failure. *Hepatology* **60**, 1346-1355 (2014).

32 Fornari, F. *et al.* MiR-221 controls CDKN1C/p57 and CDKN1B/p27 expression in human hepatocellular carcinoma. *Oncogene* **27**, 5651-5661 (2008).

33 **Cirera-Salinas, D., Pauta, M**. *et al.* Mir-33 regulates cell proliferation and cell cycle progression. *Cell Cycle* **11**, 922-933, (2012).

34 **Zhang, S.Y., Surapureddi, S**., Coulter, S., Ferguson, S.S. & Goldstein, J.A. Human CYP2C8 Is Post-Transcriptionally Regulated by MicroRNAs 103 and 107 in Human Liver. *Molecular Pharmacology* **82**, 529-540, (2012).

35 Azimifar, S.B., Nagaraj, N., Cox, J. & Mann, M. Cell-Type-Resolved Quantitative Proteomics of Murine Liver. *Cell Metabolism* **20**, 1076-1087 (2014).

36 Xiao, L. & Grove, A. Coordination of Ribosomal Protein and Ribosomal RNA Gene Expression in Response to TOR Signaling. *Current Genomics* **10**, 198-205 (2009).

37 Kimball, S.R. Eukaryotic initiation factor eIF2. *The International Journal of Biochemistry & Cell Biology* **31**, 25-29 (1999).

38 Diederichs, S. & Haber, D.A. Dual Role for Argonautes in MicroRNA Processing and Posttranscriptional Regulation of MicroRNA Expression. *Cell* **131**, 1097-1108 (2007).

39 **Gantier, M.P., McCoy, C.E.** *et al.* Analysis of microRNA turnover in mammalian cells following Dicer1 ablation. *Nucleic Acids Research* **39**, 5692-5703 (2011).

40 **Olejniczak, S.H., La Rocca, G.,** Gruber, J. J. & Thompson, C. B. Long-lived microRNA-Argonaute complexes in quiescent cells can be activated to regulate mitogenic responses. *PNAS* **110**, 157-162 (2013).

41 Runge, D.M. *et al.* Epidermal growth factor- and hepatocyte growth factor-receptor activity in serum-free cultures of human hepatocytes. *Journal of Hepatology* **30**, 265-274 (1999).

42 Yu, D. *et al.* Suppression of CYP2C9 by MicroRNA hsa-miR-128-3p in Human Liver Cells and Association with Hepatocellular Carcinoma. *Scientific Reports* **5**, 8534-8539 (2015).

43 **Wei, Z., Jiang, S**. *et al.* The Effect of microRNAs in the Regulation of Human CYP3A4: a Systematic Study using a Mathematical Model. *Scientific Reports* **4**, 1-7 (2014).

44 Li, Z. & Rana, T.M. Therapeutic targeting of microRNAs: current status and future challenges. *Nature Genetics* **13**, 622-638 (2014).

45 **Schug, J., McKenna, L.B**. *et al.* Dynamic recruitment of microRNAs to their mRNA targets in the regenerating liver. *BMC Genomics* **14**, 264 (2013).

46 Elaut, G. *et al.* Molecular mechanisms underlying the dedifferentiation process of isolated hepatocytes and their cultures. *Current Drug Metabolism* **7**, 629-660 (2006).

47 Godoy, P. *et al.* Extracellular matrix modulates sensitivity of hepatocytes to fibroblastoid dedifferentiation and transforming growth factor β-induced apoptosis. *Hepatology* **49**, 2031-2043 (2009).

48 **Bell, C.C., Hendriks, D.F., Moro, S.M.** *et al.* Characterization of primary human hepatocyte spheroids as a model system for drug-induced liver injury, liver function and disease. *Scientific Reports*, 1-13 (2016).

49 Bronevetsky, Y. *et al.* T cell activation induces proteasomal degradation of Argonaute and rapid remodeling of the microRNA repertoire. *Journal of Experimental Medicine* **210**, 417-432 (2013).

Figure 1

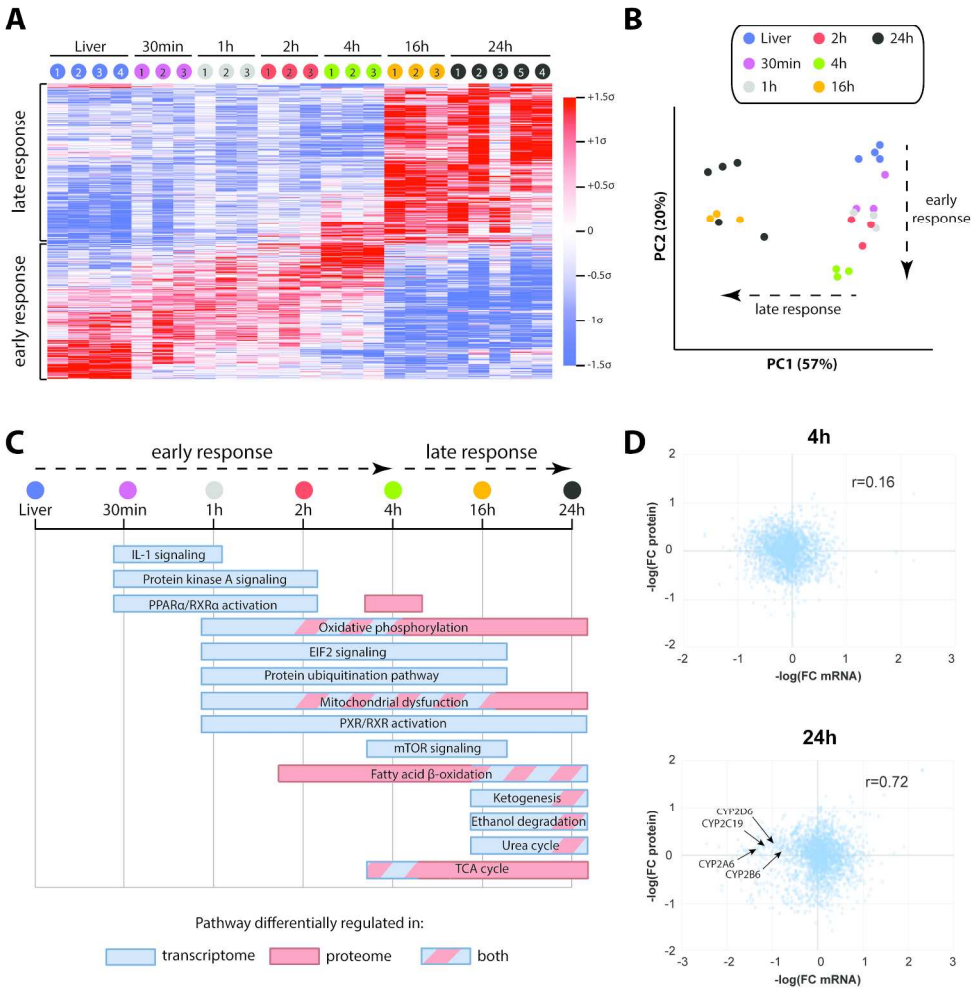

Profiling of early events in hepatic dedifferentiation on transcriptomic and proteomic level reveals overall molecular rearrangements.
Figure 1
210x226mm (300 x 300 DPI)

Figure 2

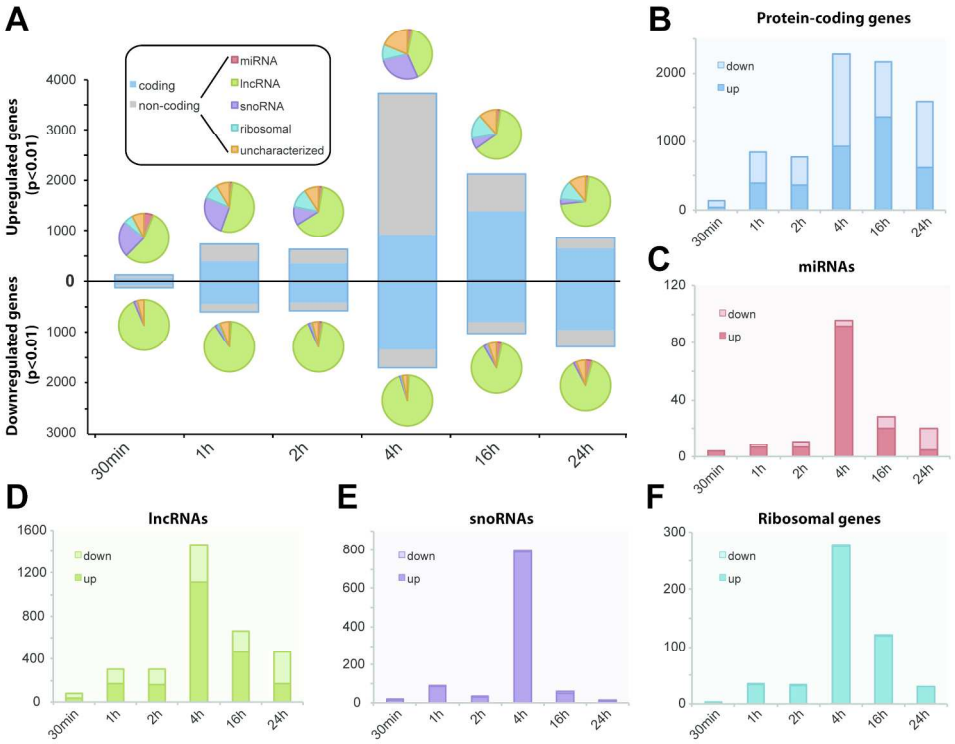

Early changes in non-coding RNAs precede rearrangements of the coding transcriptome during hepatocyte dedifferentiation.
Figure 2
210x173mm (300 x 300 DPI)

Figure 3

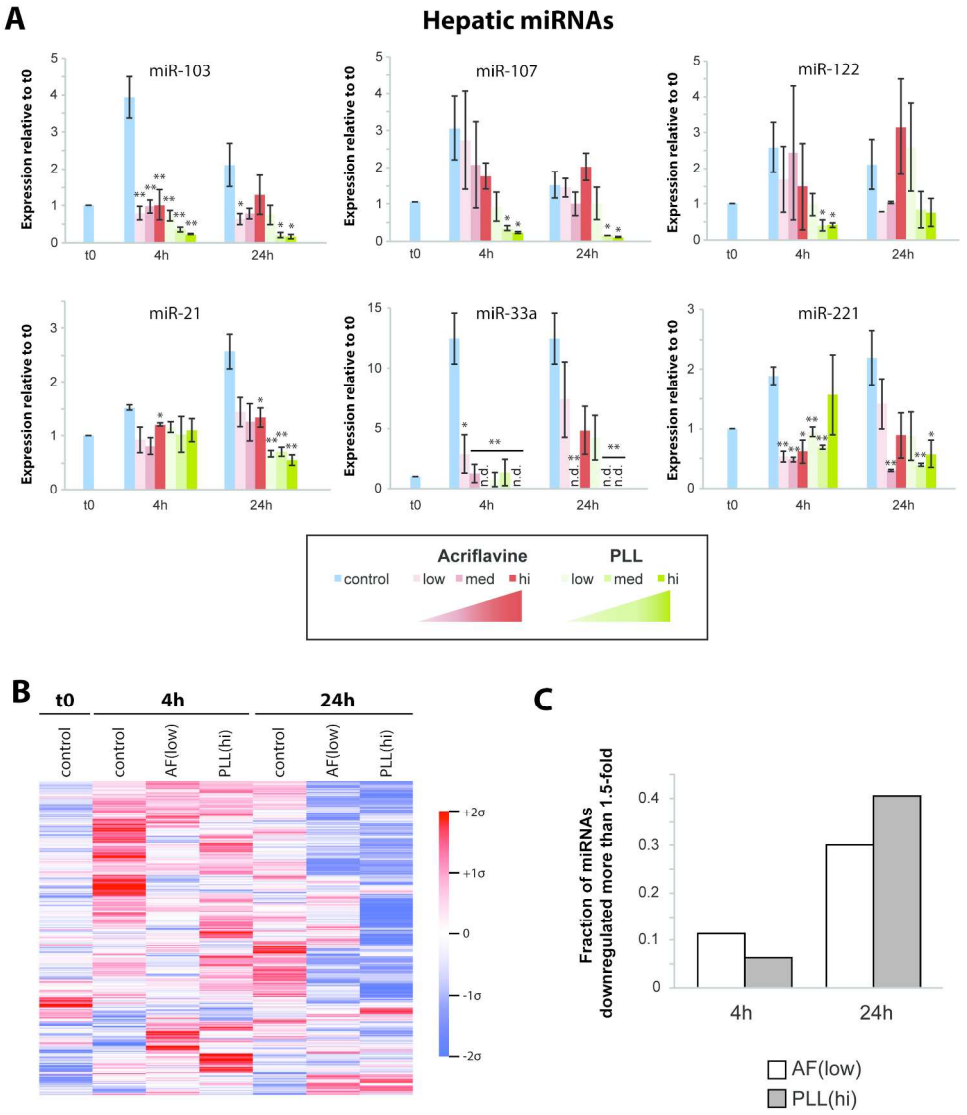

miRNA expression during hepatocyte dedifferentiation can be inhibited using small molecule inhibitors.
Figure 3
210x246mm (300 x 300 DPI)

Figure 4

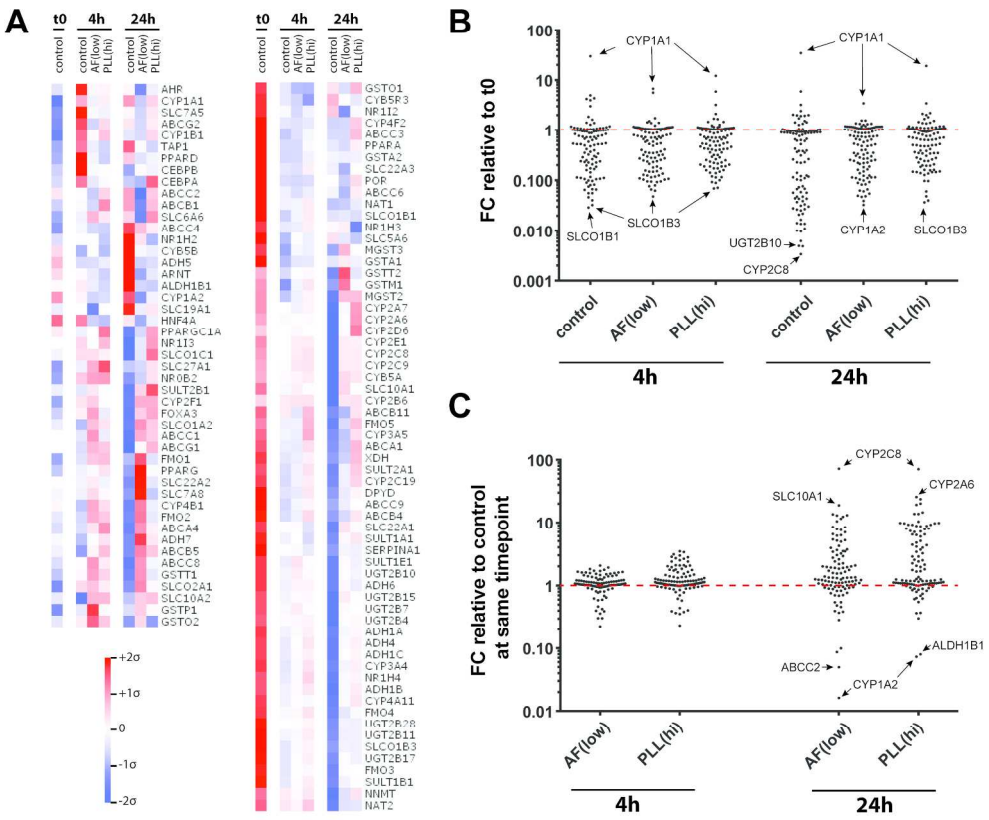

Inhibition of the miRNA machinery ameliorates changes in hepatic genes during hepatic dedifferentiation.
Figure 4
210x187mm (300 x 300 DPI)

Figure 5

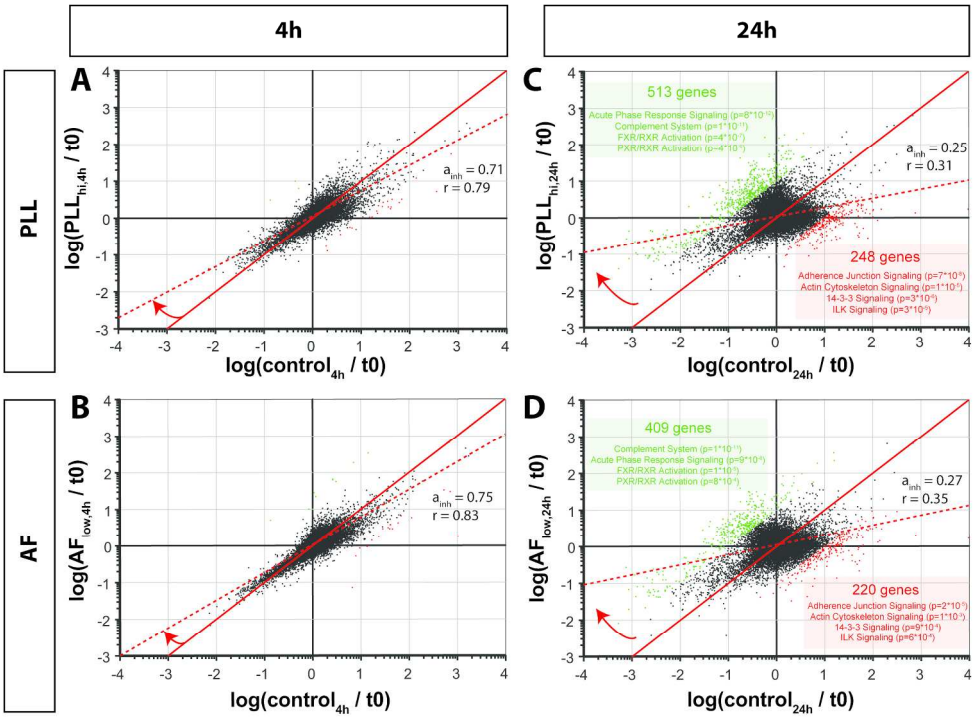

Evaluation of overall transcriptomic changes in response to miRNA inhibitors reveals drastically reduced dedifferentiation.
Figure 5
210x162mm (300 x 300 DPI)

Table 1: Demographic information of primary human hepatocyte donors used in this study.

Donor	Gender	Age	Indication	Viability of isolated cells
1	male	31	Primary scleroting cholangitis and cholangiocarcinoma	74%
2	male	36	Acute intermittent porfyria	93%
3	male	70	Colon cancer metastasis	87%
4	female	69	Colon cancer metastasis	74%
5	female	63	Colon cancer metastasis	70%

Table 2: Most differentially regulated pathways in hepatocyte dedifferentiation identified by matching changes in miRNA expression with its putative target transcripts. The table lists the top 10 KEGG pathways affected in dedifferentiation with the corresponding number of downregulated genes. Indicated p-values are obtained after correction for multiple testing. $p_{adj} \leq 0.05$ were considered significant. n.s. indicates not significantly affected pathways ($p_{adj} > 0.05$).

KEGG pathways	4h ctrl vs t0	4h PLL vs t0	4h AF vs t0
Metabolic pathways	248 ($p_{adj}=5*10^{-53}$)	139 ($p_{adj}=2*10^{-16}$)	64 ($p_{adj}=2*10^{-3}$)
Protein processing in endoplasmatic reticulum	52 ($p_{adj}=3*10^{-17}$)	37 ($p_{adj}=3*10^{-11}$)	21 ($p_{adj}=1*10^{-6}$)
Fatty acid metabolism	24 ($p_{adj}=2*10^{-14}$)	10 ($p_{adj}=1*10^{-3}$)	n.s.
Valine, leucine and isoleucine degradation	23 ($p_{adj}=4*10^{-13}$)	13 ($p_{adj}=2*10^{-5}$)	6 ($p_{adj}=0.02$)
Glycine, serine and threonine metabolism	18 ($p_{adj}=5*10^{-11}$)	7 ($p_{adj}=0.01$)	n.s.
TCA cycle	17 ($p_{adj}=2*10^{-10}$)	11 ($p_{adj}=1*10^{-5}$)	n.s.
Complement and coagulation cascades	25 ($p_{adj}=5*10^{-10}$)	10 ($p_{adj}=0.02$)	7 ($p_{adj}=0.03$)
Drug metabolism – cytochrome P450	25 ($p_{adj}=2*10^{-9}$)	11 ($p_{adj}=0.01$)	n.s.
Peroxisome	26 ($p_{adj}=2*10^{-9}$)	19 ($p_{adj}=4*10^{-6}$)	11 ($p_{adj}=3*10^{-3}$)
Tryptophan metabolism	17 ($p_{adj}=8*10^{-8}$)	8 ($p_{adj}=0.01$)	n.s.

Supporting Figure 1

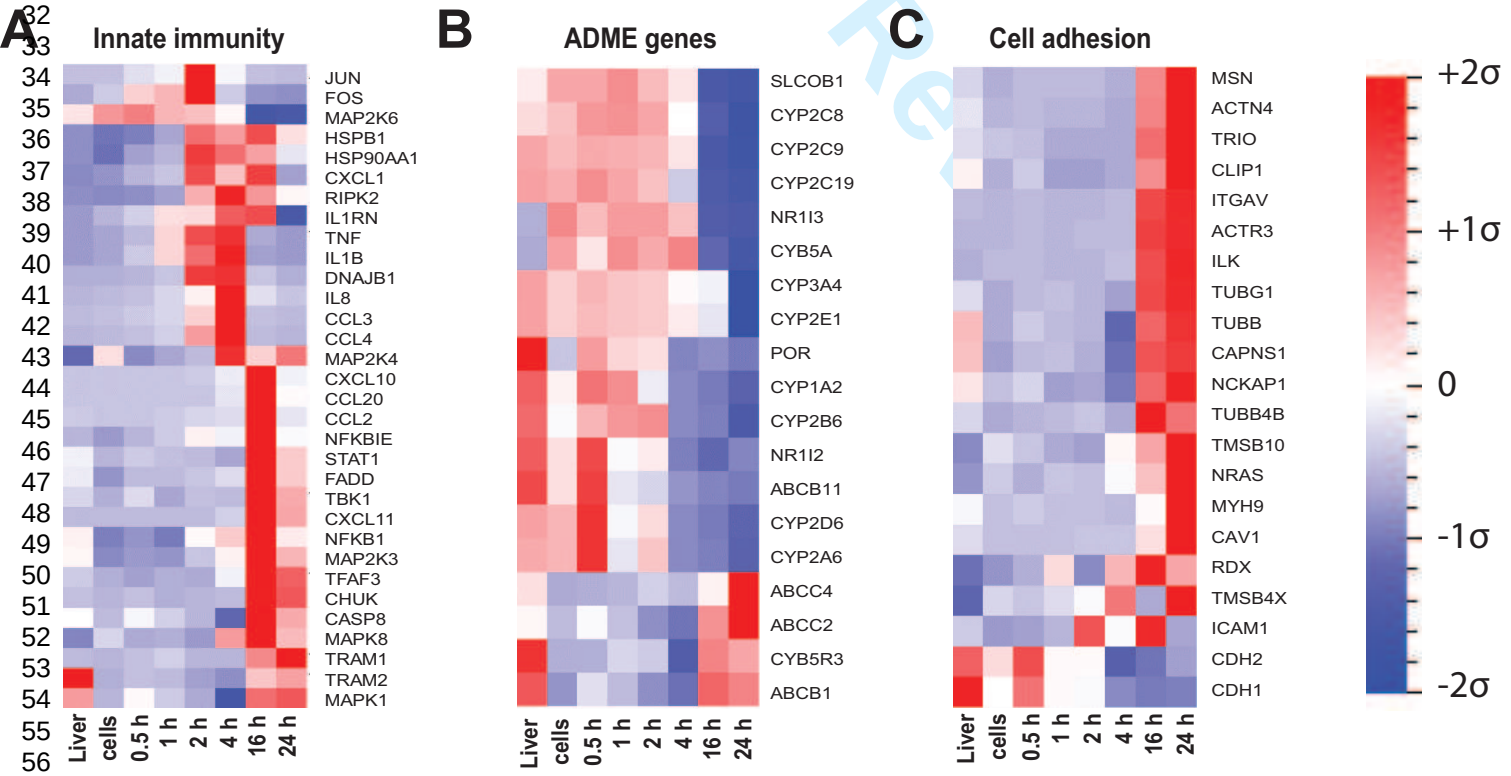

Supporting Figure 1: Expression kinetics of a selection of genes involved in innate immunity, hepatic metabolism and cell adhesion. Heatmap visualizations of mean-centred, sigma-normalized expression data of genes involved in innate immunity (**A**), drug absorption, distribution, metabolism and excretion (ADME; **B**), and cell adhesion (**C**), undergoing rapid changes upon hepatocyte dedifferentiation. Data presented are averages from primary human hepatocytes from three different individual livers.

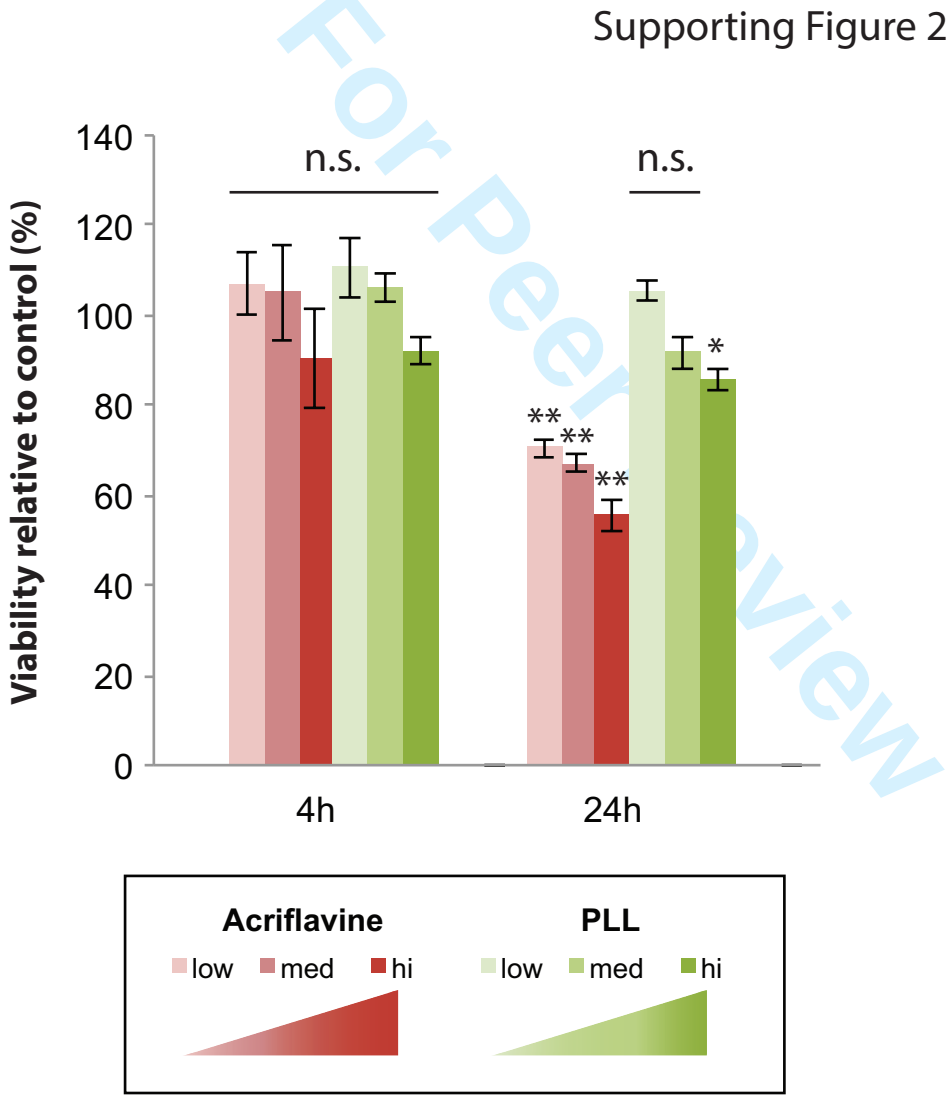

Supporting Figure 2: Impact of AF and PLL treatment on viability. Column plot showing the relative viability of samples treated with different concentrations of AF and PLL after 4 h and 24 h compared to untreated control samples at the same respective time point. N=3 experiments. Viability was determined by MTT assay. Heteroscedastic two-tailed t-tests were performed to compare treated samples with the corresponding controls at the same time point. Error bars indicate s.e. * corresponds to $p<0.05$, ** to $p<0.01$. Changes in viability were considered not significant (n.s.) when $p>0.05$.

Supporting Figure 3

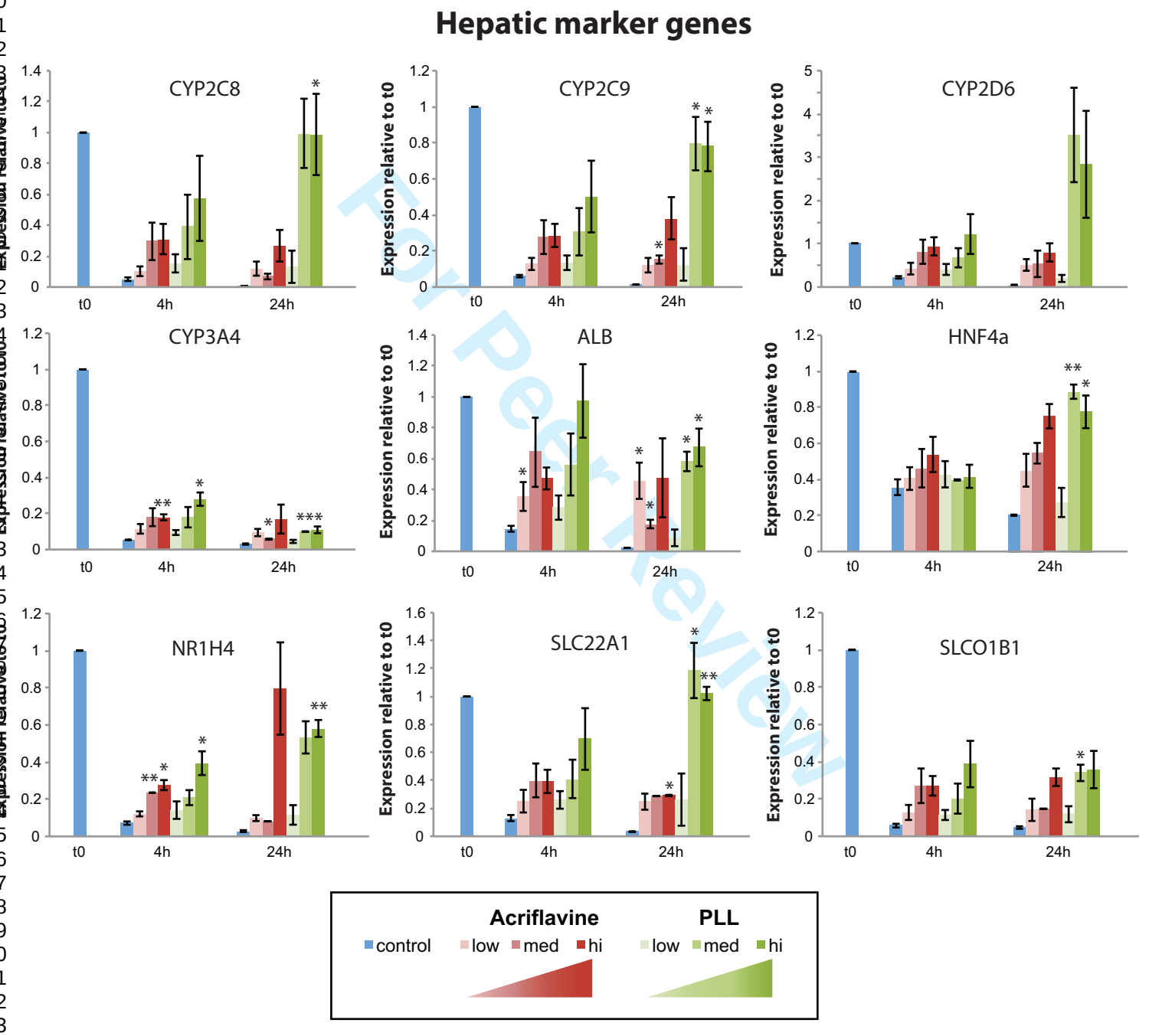

Supporting Figure 3: Inhibition of the miRNA machinery results in a delayed loss of candidate hepatic markers. The miRNA machinery was inhibited using acriflavine (AF) and poly-L-lysine (PLL). All expression levels were normalized to expression prior to dedifferentiation (t0). qRT-PCR analysis of candidate hepatic marker genes encompassing key metabolic genes (*CYP2C8*, *CYP2C9*, *CYP2D6* and *CYP3A4*), secretory products (*ALB*), hepatic transcription factors (*HNF4A*, *NR1H4*) and cellular transporters (*SLC22A1* and *SLCO1B1*) confirmed our transcriptomic results that treatment with AF or PLL increased overall expression levels of marker genes after 4 h and 24 h. N = 4 experiments. Heteroscedastic two-tailed t-tests were performed to compare inhibitor treated samples with the corresponding controls at the same time point. Error bars indicate s.e. * indicates $p<0.05$, ** indicates $p<0.01$.

Supporting Figure 4

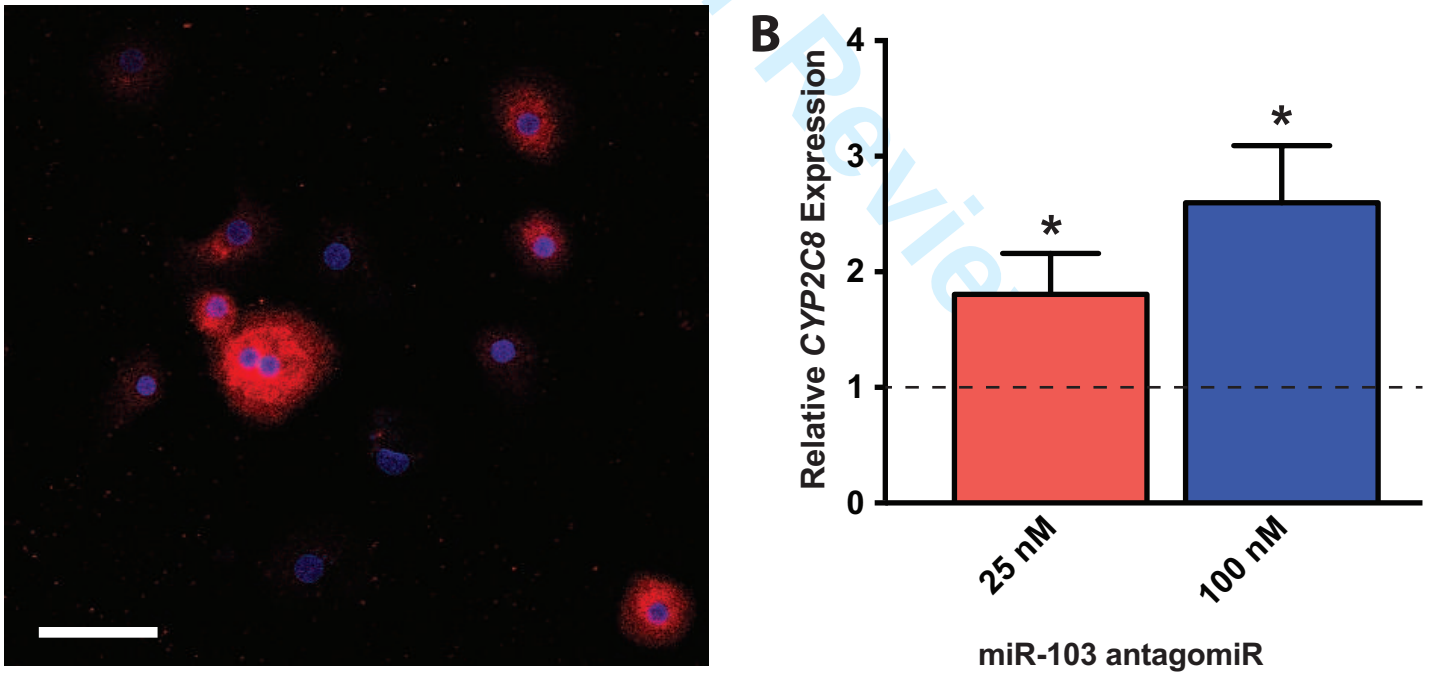

Supporting Figure 4: Downregulation of miR-103 recovers the expression of *CYP2C8* during 2D dedifferentiation. (**A**) PHH were transfected with fluorescently labeled microRNA Hairpin Inhibitor Transfection Control (Dy547 miRIDIAN, Dharmacon) and were analyzed 24 h post transfection by immunofluorescence microscopy. Scale bar = 50 µm. (**B**) PHH were transfected with miR-103 antagomiR and total RNA was isolated 24 h post transfection. Subsequently, *CYP2C8* mRNA levels were quantified by qRT-PCR and normalized to cells transfected with the control antagomiR. Note that *CYP2C8* expression was rescued dose-dependently with increasing amounts of miR-103 antagomiR. Heteroscedastic two-tailed t-tests were performed to compare antagomiR-treated samples with the controls to which they were normalized. * indicates $p<0.05$; n=3.

Supporting Figure 5

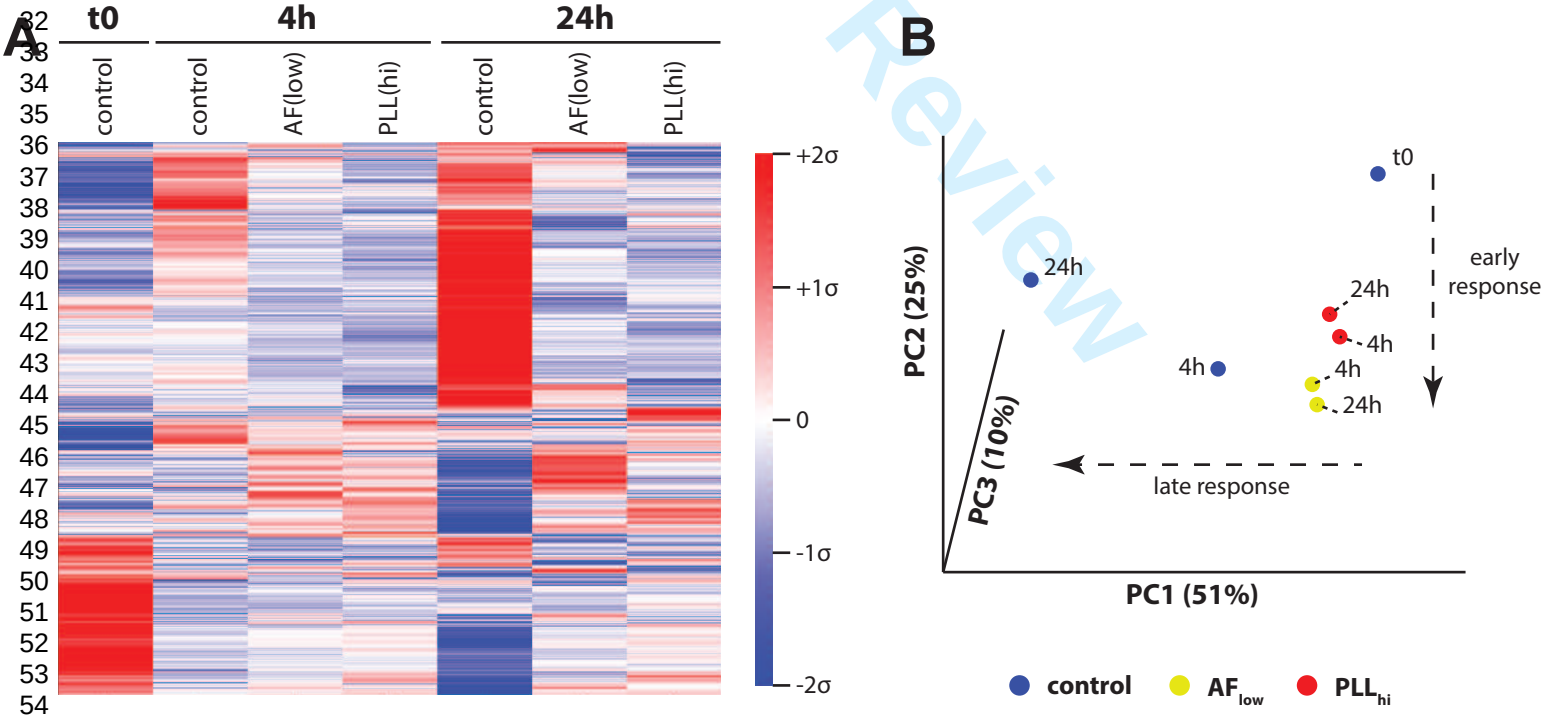

Supporting Figure 5: Effect of miRNA inhibition on genes that were found to be differentially expressed during dedifferentiation. All genes (n=4,042) that were identified as differentially expressed during hepatocyte dedifferentiation (omnibus ANOVA, FDR=0.01, see Figure 1) were included in the analysis shown. (**A**) Heatmap visualization of mean-centered, sigma-normalized expression data of differentially expressed genes upon miRNA inhibition with AF or PLL. (**B**) Principle component analysis of transcriptomic changes in control and inhibitor-treated samples. Note that while the early response is only mildly affected, progression to later stages of dedifferentiation is strongly inhibited.

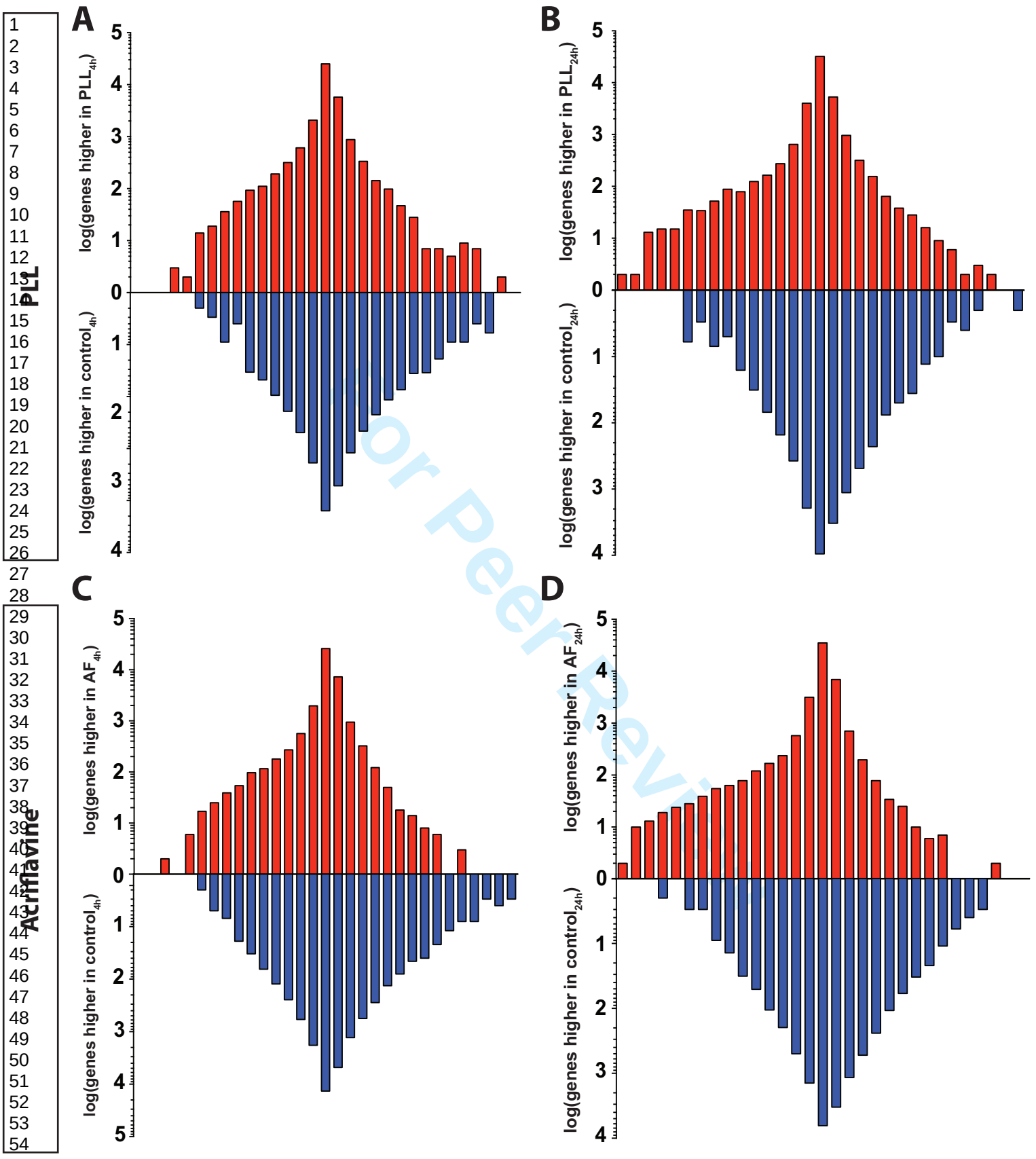

Supporting Figure 6: Inhibition of the miRNA machinery results in decreased downregulation of transcripts. Semilog-transformed histograms showing the extent of up- (red) and downregulated genes (blue) in PLL (**A**, **B**) and AF (**C**, **D**) treated samples after 4 h (**A**, **C**) and 24 h (**B**, **D**). Expression levels compared to t0 are shown on the x-axis using a bin-size of 0.2. Histograms were calculated using a rotation matrix around the control expression angle using Python. Note that the distribution of upregulated genes in AF and PLL is negatively skewed indicating an increased fraction of genes that were downregulated but to a lesser extent than in control samples consistent with a reduction of the inhibitory miRNA effect.

Supporting Methods

Materials

Cell culture medium and supplements were purchased from Sigma. Hyclone Fetal Bovine Serum (FBS) was purchased from Thermo Scientific. Acriflavine (AF, #01673) and poly-L-lysine (PLL, #P6516) were purchased from Sigma. Stock solutions were made in nuclease-free water and added directly to the culture medium.

Proteomics

Hepatocytes were washed and gently scraped into ice-cold phosphate buffer (pH 7.4) followed by centrifugation at 2000g for 5 minutes. The supernatants were discarded and the cell pellets were stored at -80°C until analysis. Each cell pellet was thawed and lysed by sonication in a volume of 0.5 M triethylammonium bicarbonate (TEAB)/0.1% sodium dodecyl sulfate (SDS) that is equivalent to cell pellet volume. The cell lysates were then centrifuged at 14,000g for 15 minutes at 4°C and the supernatants were recovered. For the liver samples, 50-100 mg of tissue per sample was homogenized in 0.5 M TEAB/0.1% SDS using a Mixer Mill 220 (Retsch, Haan, Germany) followed by sonication as per the hepatocyte samples. Protein concentrations were determined by the Bradford assay.

Prior to labelling, 100 µg of protein from each sample was reduced with 2.5 mM tris-(2-carboxyethyl) phosphine for 1 h at 60°C, alkylated with 10 mM s-methyl methanethiosulfonate (MMTS) for 10 minutes at room temperature and digested with 10 µg trypsin overnight at 37°C. The tryptic digests from each sample were labelled with one of the individual 8-plex-iTRAQ tags (iTRAQ Reagents Multiplex kit; Sciex, Framingham, Massachusetts) for 2 h at room temperature. The labelled samples were then pooled, the pH adjusted to <3 and the labelled peptides were separated on a polysulfoethyl A (200 x 4.6 mm, 5 µm, 200 Å; PolyLC Columbia, Maryland) strong cation exchange column. Cation exchange chromatography was performed on an Agilent 1100 system using Buffer A (10

mM KH_2PO_4 in 25% ACN, pH 3.0) and Buffer B (10 mM KH_2PO_4, 1 mM KCl in 25% ACN, pH 3.0) for a 95 minute gradient from 0-15% B and with a flow rate of 1 mL/minute. Collected fractions (2mL) were dried using a vacuum concentrator and resuspended in 40 µL of 0.1% formic acid prior to mass spectrometry analysis.

Peptide fractions (5 µL) were injected into an Eksigent cHiPLC Nanoflex system equipped with a trap column (C18-CL 3 µm, 0.5 mm, 120 Å) and a separation column (C18-CL 3 µm, 75 µm X 15 cm, 120 Å ChromXP). A 90 minute gradient from 2% ACN/0.1% formic acid to 50% ACN/0.1% formic acid was applied at a flow rate of 300 nL/min. MS analysis was performed on a TripleTOF 5600 system (Sciex) in positive ion mode and via information dependent acquisition.

Survey scans of 250 ms were used to trigger full-scan MS/MS acquisition of the 25 most intense ions with an accumulation time of 100 ms (total cycle time 2.8 s). A threshold for triggering of MS/MS of 100 counts per second was used, with dynamic exclusion for 12 seconds and rolling collision energy adjusted for the use of iTRAQ reagent in the Analyst method. Mass ranges of 400-1600 atomic mass units (amu) in MS and 100-1400 amu in MS/MS were used. The instrument was calibrated after every fifth sample using a beta-galactosidase digest resulting in mass accuracy of <10ppm. Data was processed using ProteinPilot 4.5 software (Sciex) and the Paragon algorithm against the latest UniProt database (release 2014_06, 20,213 human entries) with iTRAQ as a variable modification, MMTS as the cysteine alkylating reagent and biological modifications allowed. The reversed database was used as a decoy to determine the false discovery rate (FDR) for protein identification, and only those proteins identified within a 1% FDR were evaluated further. Ratios for each iTRAQ label were obtained using a pooled sample as a reference which consisted of combined aliquots of each individual sample tested.

Viability measurement

Cell viability was measured using the EZ4U cell proliferation and cytotoxicity assay (Biomedica) according to the manufacturer's instructions. 100 µl of dye

solution was added to 1 ml of sample and incubated at 37°C. After 2 h 150 µl medium was transferred to a clear 96-well plate and absorbance was measured at 450 nm and 492 nm using a microplate reader. Values were normalized against absorbance of blank medium with or without AF or PLL at the same wavelength.

Gene expression analysis

PHH were lysed directly in the culture dish and total RNA was extracted. Expression of candidate genes and miRNAs was analyzed by quantitative real-time PCR (qRT-PCR) using the TaqMan probes specified in Supporting Table 1. For miRNA analysis, RNA was reverse transcribed using either the TaqMan MicroRNA Reverse Transcription Kit (miR-103, 107, 122) or the newer TaqMan Advanced miRNA cDNA Synthesis Kit (miR-21, 22, 26a, 26b, 33a, 221; both kits from Applied Biosystems). The relative abundance of each miRNA was estimated using the ΔCt method and normalized using the housekeeping small nucleolar RNA RNU44 (miR-103, 107, 122) and miR-320a (all other miRNAs) following the manufacturers protocol. For whole transcriptome analyses, we used GeneChip Human Transcriptome Arrays 2.0 (Affymetrix) following the manufacturer's instructions.

miRNA antagomiR transfection

PHH were transfected with miRIDIAN microRNA human hsa-miR-103a-3p inhibitor or microRNA Hairpin Inhibitor Transfection Control (Dharmacon) using Lipofectamine RNAiMAX Transfection Reagent (Invitrogen) according to the manufacturer's guidelines.

Supporting Table 1: Overview of the TaqMan Assays used.

TaqMan assay	Product number (Thermo Fisher)
ALB	Hs00910225_m1
CYP2C8	Hs02383390_s1
CYP2C9	Hs02383631_s1
CYP2D6	Hs02576168_g1
CYP3A4	Hs00604506_m1
HNF4A	Hs00604431_m1
NR1H4	Hs01026590_m1
SLC22A1	Hs00427552_m1
SLCO1B1	Hs00272374_m1
TBP	Hs00427620_m1
hsa-miR-103a-3p	4427975-000439
hsa-miR-107	4427975-000443
hsa-miR-122-5p	4427975-002245
hsa-miR-22-3p	477985_mir
hsa-miR-26a-5p	477995_mir
hsa-miR-221-3p	477981_mir
hsa-miR-33a-5p	478347_mir
hsa-miR-21-5p	477975_mir
hsa-miR-26b-5p	478418_mir
hsa-miR-320a	477802_mir
RNU44 snoRNA	4427975-001094

Supporting Table 2: Overview of differentially regulated pathways and their corresponding gene constituents on transcript level. Pathways identified as differentially regulated on transcriptomic level by IPA, their p-value and the genes contained in each pathway are shown (compare Figure 1C).

Ingenuity Canonical Pathways	-log(p-value)	Molecules
30 min		
PPARa/RXRa Activation	4.19	TGFBR2, ADCY9, TGFB1, PRKAR2A, IL1B, NR2C2, MEF2C, MAP2K3, PRKAR1A
IL-1 Signaling	3.70	GNB1, ADCY9, FOS, PRKAR2A, MAP2K3, PRKAR1A
Protein Kinase A Signaling	2.68	AKAP12, GNB1, TGFBR2, ADCY9, FLNA, TGFB1, PTPRB, PRKAR2A, PRKAR1A
1h		
EIF2 Signaling	6.65	PABPC1, PIK3CA, RPL17, RPS10, EIF4G3, RPS21, EIF2S3, EIF4A2, RPL26, EIF3E, EIF4G1, EIF2A, FAU, RPL9, RPL27, RPL27A, RPL8, RPL18A, EIF3B, EIF3I, RPL19, RPL21, RPS27A, INSR, RPL18, RPL13A, EIF3K
Oxidative Phosphorylation	6.25	SDHA, ATP5G1, COX7B, ATP5H, NDUFA7, COX6A1, COX5B, NDUFB5, ATP5L, SDHC, NDUFA2, NDUFB3, ATP5C1, NDUFB9, NDUFA6, NDUFB6, NDUFS2, NDUFA12, NDUFS3, ATP5F1
Protein Ubiquitination Pathway	5.68	USP24, DNAJB4, UBR2, UBE3B, SKP1, DNAJC8, HSPE1, USP47, PSMA2, AMFR, PSMA6, USP15, UBE2Q1, UBE4B, PSMD13, DNAJC19, USP9X, BIRC6, PSMA1, PSMD8, PSMB7, PSME1, UBE2H, USP32, USP22, DNAJB11, PSMA5, UBR1, BAP1, USP34, BIRC2
Mitochondrial Dysfunction	5.05	SDHA, ATP5G1, FURIN, COX7B, ATP5H, NDUFA7, COX6A1, COX5B, NDUFB5, ATP5L, SDHC, VDAC3, NDUFB3, NDUFA2, APP, ATP5C1, NDUFB9, PRDX3, NDUFA6, NDUFB6, NDUFS2, NDUFA12, NDUFS3, ATP5F1, PINK1
PPARa/RXRa Activation	2.33	GNAS, GNAQ, NR2C2, MED12, ABCA1, NCOA3, PRKAG1, TGFBR2, ADCY9, TGFB1, PRKACA, IL1B, MEF2C, NCOR1, MAP2K3, INSR, RXRA, MAP4K4, PRKAR1A
IL-1 Signaling	1.69	GNAI2, GNB1, ADCY9, IL1A, GNAS, PRKACA, GNAQ, MAP2K3, PRKAG1, PRKAR1A
Protein Kinase A Signaling	1.53	AKAP12, FLNB, PTPRK, GNAS, YWHAE, GNAQ, PRKAG1, PTPRF, AKAP11, ROCK1, YWHAQ, ROCK2, GNAI2, TGFBR2, AKAP2, GNB1, ADCY9, PTPN11, TGFB1, PTPRB, PRKACA, ADD1, PRKAR1A, DUSP16
PXR/RXR Activation	1.43	PRKACA, ABCB11, INSR, RXRA, ABCC3, PAPSS2, PRKAG1, SLCO1B3, PRKAR1A
2h		
Oxidative Phosphorylation	3.97	SDHA, SDHB, NDUFA9, ATP5H, COX6A1, COX5B, NDUFB5, ATP5L, NDUFA2, ATP5C1, NDUFA6, NDUFA12, NDUFS3, ATP5F1, ATP5G3
Protein Ubiquitination Pathway	3.67	USP24, UBE4B, USP15, DNAJB4, PSMD13, UBR2, UBE3B, USP9X, DNAJC12, BIRC6, PSMA1, PSMD8, PSMB7, PSME1, USP32, UBE2B, USP22, DNAJC8, USP47, HSPE1, PSMB1, BAP1, USP34, BIRC2
Mitochondrial	3.61	SDHA, FURIN, SDHB, ATP5H, NDUFA9, COX6A1, COX5B,

Dysfunction		NDUFB5, ATP5L, BACE1, NDUFA2, APP, ATP5C1, PRDX3, NDUFA6, NDUFA12, NDUFS3, ATP5F1, ATP5G3, PINK1
EIF2 Signaling	3.06	PIK3CA, RPL17, RPS10, EIF4G3, EIF4A2, EIF4G1, EIF2A, FAU, RPL8, RPL35, EIF1, RPL18A, EIF3I, RPL19, INSR, RPL18, ATM, EIF3K
PPARa/RXRa Activation	2.64	CD36, GNAQ, PRKAR2A, NR2C2, IL6, MED12, ABCA1, NCOA3, PRKAG1, TGFBR2, ADCY9, TGFB1, MEF2C, NCOR1, INSR, RXRA, MAP4K4, PRKAR1A
Protein Kinase A Signaling	2.53	AKAP12, FLNB, PTPRK, YWHAE, PDE3A, GNAQ, PRKAR2A, ANAPC13, PHKA2, PTPRF, PRKAG1, AKAP11, TGFBR2, YWHAQ, ROCK2, GNB1, AKAP2, ADCY9, NFAT5, PTPN11, TGFB1, PTPRB, ADD1, PPP3CA, PRKAR1A
PXR/RXR Activation	1.36	PRKAR2A, ABCB11, INSR, IL6, RXRA, ABCC3, PRKAG1, PRKAR1A
4h		
Mitochondrial Dysfunction	9.69	MAP2K4, FURIN, XDH, ACO2, NDUFB5, ATP5L, NCSTN, NDUFA1, NDUFB3, PDHA1, MAOB, NDUFS1, ATP5F1, NDUFS7, ATP5A1, BACE1, SDHC, UQCR11, ATP5C1, PRDX3, NDUFA6, NDUFB7, VDAC1, NDUFS3, ATP5G1, COX7B, SDHB, ATP5H, COX6A1, NDUFA7, NDUFA2, NDUFB9, ATP5J2, NDUFS2, NDUFB6, OGDH, CASP8, AIFM1, NDUFS4, SDHA, NDUFV1, COX6B1, GLRX2, MAPK8, VDAC3, APP, NDUFV2, COX7A2, SDHD, CYCS, PINK1, PSEN1, MAOA
EIF2 Signaling	9.20	RPL11, RAF1, MAPK1, RPL39, EIF2A, EIF3B, EIF4G2, RPL19, RPL21, ATM, PABPC1, EIF2AK1, RPL29, EIF4G3, RPL12, EIF3E, RPL37A, RPL9, RPL15, RPL8, INSR, RPL41, RPL13A, EIF3K, PIK3CA, RPS3A, RPL26, EIF4G1, RPL27A, RPL35, RPL18A, EIF3A, RPS3, RPS5, RPL31, RPL18, RPS24, GRB2, RPL17, RPS10, RPS21, RPS29, FAU, RPL27, EIF3G, RPS26, RPS27A, RPL37, EIF3L, RPL38
Oxidative Phosphorylation	6.84	SDHB, COX7B, ATP5G1, ATP5H, COX6A1, NDUFA7, NDUFB5, ATP5L, NDUFA1, NDUFB3, NDUFA2, NDUFB9, NDUFS1, ATP5J2, NDUFS2, NDUFB6, ATP5F1, NDUFS4, SDHA, NDUFV1, COX6B1, NDUFS7, ATP5A1, SDHC, UQCR11, ATP5C1, NDUFV2, NDUFA6, NDUFB7, COX7A2, SDHD, CYCS, NDUFS3
Protein Ubiquitination Pathway	5.25	USP45, PSMA7, UBE3B, UBR2, DNAJC15, SKP1, UBE2B, USP10, PSMA2, PSMA6, DNAJB12, UBE4B, UBE2Q1, USP9X, DNAJC19, PSMD5, BIRC6, PSMB7, USP32, PSMB2, UBR1, BAP1, PSMB1, ANAPC5, DNAJB6, UBE2E1, USP24, USP12, UBE2N, DNAJC12, ANAPC10, CDC23, HSP90B1, HSPE1, USP16, USP47, PSMA3, PSMD14, AMFR, USP15, UBE2R2, PSMA1, DNAJB9, PSMD8, UBE2J1, USP4, DNAJB11, USP22, PSMD2, BTRC, USP34, UBE2D3, BIRC2
TCA Cycle	2.36	SDHA, SDHB, SUCLG1, ACO2, SDHD, SDHC, MDH1, OGDH, IDH3B
PXR/RXR Activation	1.52	PPARA, PRKAR2A, CES2, HMGCS2, UGT1A1, PAPSS2, ALDH1A1, ALDH3A2, PRKACA, NCOA1, ABCB11, INSR, RXRA, ABCC3, TNF, SLCO1B3, PRKAR1A
mTOR Signaling	1.45	TSC1, PIK3CA, MAPK1, RPS3A, PPP2CA, EIF4G1, PRR5L, PDGFC, MTOR, EIF3B, EIF4G2, TSC2, EIF3A, RPS3, RPS5, EIF4B, ATM, RPS24, RHEB, STK11, RPS10, EIF4G3, RPS21, EIF3E, RPS29, PPP2R5A, FAU, EIF3G, RPS26, RPS27A, INSR, EIF3L, EIF3K
16h		
EIF2 Signaling	16.90	RPL11, RPL39, KRAS, EIF4A2, EIF2A, EIF1, EIF4G2, EIF3D, PAIP1, EIF5, RPL21, RPL19, RPS2, RPL36AL, RPL29, RPL12, EIF2S3, EIF3E, RPL37A, RPL28, RPL9, RPL15, RPL8, INSR, RPL13A, RPL41, EIF3K, RPSA, RPLP1, RPS3A, RPS18, RPL26,

		RPL7, RPS4X, RPL27A, RPL35, RPL18A, RPS17, RPS3, RPS5, RPL31, RPL18, RPS24, RPL4, NRAS, EIF3H, RPL17, RPS10, RPL30, EIF3J, RPS21, RPS29, FAU, EIF3G, RPL27, RRAS2, RPS26, EIF3I, RPS27A, RPL37, RPL38, RPLP0
Protein Ubiquitination Pathway	6.04	USP45, PSMA7, UBR2, SKP1, HSPA5, TCEB1, UCHL5, NEDD4L, PSMB5, UBE4B, USP9X, HSPA9, PSMD5, PSMC4, BIRC6, PSMD6, DNAJC2, PSMB7, PSMD11, UBE2L3, PSMA5, PSMD12, PSMB1, ANAPC5, PSMA4, HSP90AA1, PSMD4, UBE2E1, USP24, USP12, USP14, PSMD7, UBE2N, PSMD9, UBE2F, USP3, PSMD10, HSPE1, USP16, PSMA3, PSMD14, HSPA4L, PSMB4, UBE2M, PSMD13, DNAJC1, PSMA1, HSPD1, DNAJB9, PSMD8, PSMD2, CDC34, USP25, DNAJC7, BIRC2
mTOR Signaling	4.26	RPS3A, PPP2CA, RPS18, KRAS, EIF4A2, PDGFC, PRKAG1, RPS4X, EIF4EBP1, EIF4G2, EIF3D, TSC2, RPS2, RPS17, RPS5, RPS3, PRKD3, RPS24, RPS6KB1, RHEB, NRAS, EIF3H, RPS10, EIF3J, RPS21, EIF3E, RPS29, PLD1, PPP2R5A, FAU, EIF3G, PPP2CB, PPP2R1A, RRAS2, PRKCI, RHOQ, RPS26, EIF3I, RPS27A, INSR, EIF3K, RPSA, PRKCB
Fatty Acid b-oxidation I	3.72	ACAA1, ACAA2, SCP2, ACSL5, AUH, HADHB, IVD, EHHADH, ACADM, HSD17B4, HADH, HADHA, ACSL1
Ethanol Degradation II	3.02	ADH6, ALDH2, ADH1A, ALDH3A2, ADH1C, ADH1B, PECR, ALDH9A1, ACSL1, ADH4
PXR/RXR Activation	2.99	PPARA, CYP3A7, GSTA2, CYP2C9, CES2, HMGCS2, UGT1A1, PRKAG1, PAPSS2, SULT2A1, ALDH3A2, PRKACA, ABCB11, G6PC, INSR, RXRA, ABCC3, TNF, SLCO1B3, PRKAR1A, CYP2C8
Mitochondrial Dysfunction	2.37	MAP2K4, FURIN, ATP5G1, NDUFA9, COX6A1, NDUFA7, XDH, NCSTN, NDUFA2, VDAC2, PDHA1, NDUFS1, MAOB, NDUFB9, SOD2, NDUFS2, HTRA2, CASP8, COX4I1, AIFM1, NDUFA8, SDHA, NDUFV1, GLRX2, MAPK8, BACE1, VDAC3, APP, ATP5C1, NDUFA6, CAT, CYC1, CYCS, MAOA, PINK1
Ketogenesis	2.10	BDH1, HADHB, HMGCL, HMGCS2, HADHA
Urea Cycle	1.31	OTC, CPS1, ARG1
24h		
Fatty Acid b-oxidation I	10.20	HSD17B10, SLC27A2, ACAA1, ACAA2, HSD17B8, SLC27A5, SCP2, ECI2, ACSL5, AUH, HADHB, EHHADH, IVD, ACADM, HSD17B4, HADHA, ACSL1, HADH
Ethanol Degradation II	7.11	HSD17B10, ADH6, ALDH2, ADH1A, ALDH4A1, AKR1A1, ALDH3A2, ADH1C, ADH1B, PECR, ACSL1, ALDH9A1, ADH4
PXR/RXR Activation	5.54	PPARA, CYP3A7, GSTA2, CYP2C9, CES2, HMGCS2, UGT1A1, PRKAG1, SULT2A1, CYP1A2, CYP3A4, PCK2, ALDH3A2, NR1I3, ABCB11, GSTA1, G6PC, TNF, SLCO1B3, PPARGC1A, CYP2C8, PRKAR1A
Ketogenesis	3.82	BDH1, ACAT1, HADHB, HMGCL, HMGCS2, HADHA
Urea Cycle	2.79	OTC, ASL, CPS1, ARG1

Supporting Table 3: Overview of differentially regulated pathways and their corresponding gene constituents on protein level. Pathways identified as differentially regulated on proteomic level by IPA, their p-value and the genes contained in each pathway are shown (compare Figure 1C). For proteomic analyses, a fold-change threshold of 2 was applied.

Ingenuity Canonical Pathways	-log(p-value)	Molecules
2h		
Fatty Acid b-oxidation I	7.23	ACAA1, SCP2, ECI2, EHHADH, ACAA2, ECI1, HADH
Mitochondrial Dysfunction	5.72	ATP5J, SDHB, PRDX3, NDUFS1, SOD2, ATP5H, ATP5D, PARK7, TXN2, NDUFS2, UQCRFS1
Oxidative Phosphorylation	4.00	ATP5J, SDHB, NDUFS1, ATP5H, ATP5D, NDUFS2, UQCRFS1
4h		
Mitochondrial Dysfunction	11.30	SDHA, ATP5J, NDUFV1, ATP5H, ATP5D, COX5B, NDUFA2, NDUFS1, PRDX3, SOD2, NDUFV2, TXN2, ATP5J2, UQCRFS1, NDUFS2, CYCS, CYB5A, UQCRC1, ACO1, AIFM1, MAOA
Oxidative Phosphorylation	9.37	SDHA, ATP5J, NDUFV1, NDUFS1, ATP5H, NDUFV2, ATP5D, COX5B, ATP5J2, NDUFS2, UQCRFS1, CYCS, CYB5A, UQCRC1, NDUFA2
Fatty Acid b-oxidation I	8.10	ACAA1, SCP2, ECI2, HADHB, HSD17B4, ACAA2, ECI1, HADHA, HADH
TCA Cycle	3.96	SDHA, DHTKD1, DLST, MDH2, ACO1
PPARa/RXRa Activation	1.33	HSP90B1, GPD1, ACAA1, HSP90AB1, PDIA3, FASN, GOT2
24h		
Mitochondrial Dysfunction	9.82	HSD17B10, SDHA, ATP5J, NDUFV1, ATP5H, ATP5D, COX5B, ATP5A1, NDUFS1, PRDX3, SOD2, NDUFS8, NDUFV2, PARK7, UQCRFS1, NDUFS2, CYCS, UQCRC1, ACO1, NDUFS3, MAOA, AIFM1
Ethanol Degradation II	9.76	ADH6, ADH5, HSD17B10, ALDH4A1, ADH1A, AKR1A1, ALDH1A1, ADH1C, ADH1B, ADH4
Oxidative Phosphorylation	7.69	SDHA, ATP5J, NDUFV1, ATP5H, ATP5D, COX5B, ATP5A1, NDUFS1, NDUFV2, NDUFS8, NDUFS2, UQCRFS1, CYCS, UQCRC1, NDUFS3
Urea Cycle	5.14	OTC, ASS1, ASL, ARG1
TCA Cycle	4.48	SDHA, DLST, DLD, MDH1, MDH2, ACO1
Fatty Acid b-oxidation I	2.81	HSD17B10, ACAA1, HADHB, ACAA2, ECI1
Ketogenesis	2.67	ACAT2, ACAT1, HADHB

Supporting Table 4: Overview of affected pathways under AF and PLL treatment after 24 hours. Pathways identified as differentially regulated by IPA, their p-value and the genes contained in each pathway are shown (compare Figure 4C,D). Only genes that changed >10-fold were considered. Only pathways that were significant after correction for multiple testing are shown (FDR=0.05).

Ingenuity Canonical Pathways	-log(p-value)	Molecules
Upregulated in PLL		
Acute Phase Response Signaling	11.10	HAMP, HPX, ITIH3, C3, C9, CP, C5, PLG, KLKB1, FOS, MBL2, ITIH2, APCS, ITIH4, CRP, A2M
Complement System	10.70	MBL2, C3, C9, CFI, C8B, C6, CFH, C8A, C5
Coagulation System	7.24	F11, PLG, KLKB1, SERPINC1, F9, F5, A2M
FXR/RXR Activation	6.31	PON1, HPX, C3, APOF, ITIH4, C9, ABCB11, G6PC, PON3, PPARGC1A
PXR/RXR Activation	5.35	ABCB11, CYP2A6 (includes others), G6PC, IGFBP1, HMGCS2, CYP2C8, PPARGC1A
Intrinsic Prothrombin Activation Pathway	5.21	F11, KLKB1, SERPINC1, F9, F5
LPS/IL-1 Mediated Inhibition of RXR Function	4.75	CAT, ABCB11, FABP1, CYP2A6 (includes others), HMGCS2, CYP4A11, ACSL1, ABCA1, CYP2C8, PPARGC1A
LXR/RXR Activation	4.67	PON1, HPX, C3, APOF, ITIH4, C9, PON3, ABCA1
Systemic Lupus Erythematosus Signaling	3.02	FOS, C9, C8B, C6, C8A, C5
Urea Cycle	2.86	CPS1, ARG1
Histidine Degradation III	2.86	HAL, AMDHD1
Ethanol Degradation II	2.86	ADH1B, ACSL1, ADH4
Histidine Degradation VI	2.69	HAL, AMDHD1
Upregulated in AF		
Complement System	10.70	MBL2, C9, CFI, C8B, C6, CFH, C8A, C5
Acute Phase Response Signaling	7.03	HAMP, PLG, MBL2, ITIH2, APCS, ITIH4, C9, CRP, A2M, C5
Serotonin Degradation	6.34	ADH6, UGT2B7, ADH1B, UGT2B10, ADH4, UGT2B15
FXR/RXR Activation	4.84	PON1, SLC10A1, APOF, ITIH4, C9, G6PC, PON3
Coagulation System	4.10	PLG, SERPINC1, F9, A2M
Nicotine Degradation III	3.61	UGT2B7, UGT2B10, CYP2C8, UGT2B15
Melatonin Degradation I	3.61	UGT2B7, UGT2B10, CYP2C8, UGT2B15
Superpathway of Melatonin Degradation	3.49	UGT2B7, UGT2B10, CYP2C8, UGT2B15
Ethanol Degradation II	3.44	ADH6, ADH1B, ADH4
Nicotine Degradation II	3.42	UGT2B7, UGT2B10, CYP2C8, UGT2B15
Thyroid Hormone Metabolism II (via Conjugation and/or Degradation)	3.30	UGT2B7, UGT2B10, UGT2B15
Urea Cycle	3.25	CPS1, ARG1
Noradrenaline and Adrenaline Degradation	3.24	ADH6, ADH1B, ADH4
Systemic Lupus Erythematosus Signaling	3.12	C9, C8B, C6, C8A, C5
PXR/RXR Activation	3.06	G6PC, IGFBP1, HMGCS2, CYP2C8

LXR/RXR Activation	3.06	PON1, APOF, ITIH4, C9, PON3
Maturity Onset Diabetes of Young (MODY) Signaling	2.45	SLC2A2, FABP1
Superpathway of Citrulline Metabolism	2.38	CPS1, ARG1
4-hydroxybenzoate Biosynthesis	2.12	TAT
4-hydroxyphenylpyruvate Biosynthesis	2.12	TAT
Downregulated in PLL		
Epithelial Adherens Junction Signaling	4.61	CDH2, CDH1, ACTR3, NRAS, MYH9, TUBB4B, TUBG1, TGFB2, ACTN4, TUBB, CLIP1
14-3-3-mediated Signaling	3.43	YWHAQ, NRAS, TUBB4B, TUBG1, YWHAZ, GSK3B, PDCD6IP, SFN, TUBB
Remodeling of Epithelial Adherens Junctions	3.43	CDH1, ACTR3, TUBB4B, TUBG1, ACTN4, TUBB, CLIP1
tRNA Charging	3.42	NARS, GARS, KARS, FARSB, FARSA
Sertoli Cell-Sertoli Cell Junction Signaling	3.19	CDH1, NRAS, TUBB4B, ZAK, TUBG1, ILK, GSK3B, ACTN4, TUBB, OCLN
Actin Cytoskeleton Signaling	3.19	ACTR3, NRAS, MYH9, FGF2, RDX, TRIO, ACTN4, TMSB10/TMSB4X, MSN, NCKAP1
RAN Signaling	3.09	KPNB1, KPNA3, CSE1L, KPNA2
ILK Signaling	2.95	FLNB, RELA, CDH1, PPP2R1A, MYH9, ILK, GSK3B, ACTN4, TMSB10/TMSB4X
Germ Cell-Sertoli Cell Junction Signaling	2.87	CDH2, CDH1, NRAS, TUBB4B, TUBG1, ILK, TGFB2, ACTN4, TUBB
PI3K/AKT Signaling	2.56	YWHAQ, RELA, PPP2R1A, NRAS, YWHAZ, ILK, GSK3B, SFN
Integrin Signaling	1.72	ACTR3, NRAS, CAPNS1, ITGAV, CAV1, ILK, GSK3B, ACTN4
Myc Mediated Apoptosis Signaling	1.66	YWHAQ, NRAS, YWHAZ, SFN, FAS
Wnt/b-catenin Signaling	1.49	CDH2, CDH1, PPP2R1A, CSNK2A1, ILK, TGFB2, GSK3B
Cyclins and Cell Cycle Regulation	1.49	PPP2R1A, PA2G4, CDK6, TGFB2, GSK3B
p70S6K Signaling	1.47	YWHAQ, PPP2R1A, NRAS, EEF2, YWHAZ, SFN
Aryl Hydrocarbon Receptor Signaling	1.47	ALDH1B1, RELA, CYP1A2, NQO1, CDK6, TGFB2, FAS
HIPPO signaling	1.47	YWHAQ, PPP2R1A, YWHAZ, MOB1A, SFN
Regulation of Cellular Mechanics by Calpain Protease	1.43	NRAS, CAPNS1, CDK6, ACTN4
Regulation of the Epithelial-Mesenchymal Transition Pathway	1.43	RELA, CDH2, CDH1, NRAS, FGF2, TGFB2, GSK3B
Downregulated in AF		
tRNA Charging	3.09	NARS, LARS, GARS, FARSB, EPRS
Remodeling of Epithelial Adherens Junctions	2.63	CDH1, ACTR3, TUBB4B, ACTN4, TUBB, CLIP1
Epithelial Adherens Junction Signaling	2.63	CDH2, CDH1, ACTR3, MYH9, TUBB4B, ACTN4, TUBB, CLIP1
Sertoli Cell-Sertoli Cell Junction Signaling	2.63	SPTBN1, CDH1, TUBB4B, ZAK, ILK, GSK3B, ACTN4, TUBB, OCLN
RAN Signaling	1.62	KPNB1, KPNA3, CSE1L
ILK Signaling	1.57	FLNB, CDH1, PPP2R1A, MYH9, ILK, GSK3B, ACTN4
14-3-3-mediated Signaling	1.48	TUBB4B, YWHAZ, GSK3B, PDCD6IP, SFN, TUBB

Actin Cytoskeleton Signaling	1.36	ROCK2, ACTR3, MYH9, FGF2, TRIO, ACTN4, MSN